Impact of global change on ocean biogeochemical cycles (N, P, C and trace elements)
Palma de Mallorca, 4 – 8 Nov 2013

I. Micro-nutrients in the oceans

X. Antón Álvarez Salgado

CSIC, Instituto de Investigacións Mariñas

C/ Eduardo Cabello 6, 36208 - Vigo

http://www.iim.csic.es

outline of this presentation

some general concepts

Seawater…

… is a medium of high ionic strenght

$$I = 0,5 \cdot \Sigma(C_i \cdot Z_i^2) \sim 19,92 \cdot S/(1000-1.005 \cdot S) \sim 0.7 \text{ mol/kg}$$

$$a_C = f_c(I) \cdot [C]$$

… that experiences hidrostatic pressures ranging from 1 to 1000 atm

($\Delta P / \Delta z \sim 0.1$ atm/m)

$$\frac{d(\ln K)}{dP} = -\frac{\Delta V_i}{R \cdot T}$$ (↑P, ↑ K cause ions occupy less volume)

$$\frac{d(\ln k)}{dP} = -\frac{\Delta V_i}{R \cdot T}$$ (↑P, ↑ k cause ions occupy less volume)

outline of this presentation

some general concepts

Seawater…

… is a medium that experiences temperatures ranging from -2°C to >30°C

$$\frac{d(\ln K)}{dT} = \frac{\Delta H^0}{R \cdot T^2}$$

(Vant Hoff law, free entalpy)

($\Delta H^0 > 0$, ↑T ↑K; $\Delta H^0 < 0$, ↑T ↓K)

$$\frac{d(\ln k)}{dT} = \frac{\Delta G^{\perp 0}}{R \cdot T^2}$$

(Arhenius law, free activation energy > 0, ↑T ↑k)

outline of this presentation

some general concepts

Seawater…

… is a buffer solution

$$CO_2 + H_2O \overset{K_1}{\Leftrightarrow} HCO_3^- + H^+$$

$$HCO_3^- \overset{K_2}{\Leftrightarrow} CO_3^{2-} + H^+$$

$$H_3BO_3 + H_2O \overset{K_B}{\Leftrightarrow} B(OH)_4^- + H^+$$

STANDARD SEAWATER

(pHsws = 8.0; $\sum CO_2$ = 2100 µmol ·kg^{-1})

K_1(35, 15) = $10^{-6.04}$	[CO_2] = 13.8 µmol ·kg^{-1} (0.7%)
K_2(35,15) = $10^{-9.23}$	[HCO_3^-] = 1916.5 µmol ·kg^{-1} (91.3%)
α_S(35,15) = $10^{-1.43}$	[CO_3^{2-}] = 169.6 µmol ·kg^{-1} (8.0%)
K_B(35, 15) = $10^{-8.74}$	[$B(OH)_4^-$] = 88.7 µmol ·kg^{-1} (21.3%)
	[H_3BO_3] = 327.7 µmol ·kg^{-1} (78.7%)

outline of this presentation

some general concepts

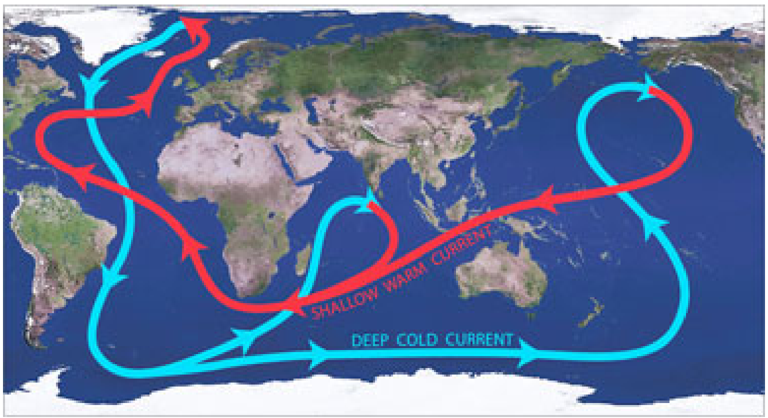

global conveyor belt

outline of this presentation

C, N P and Si reservoirs in the oceans

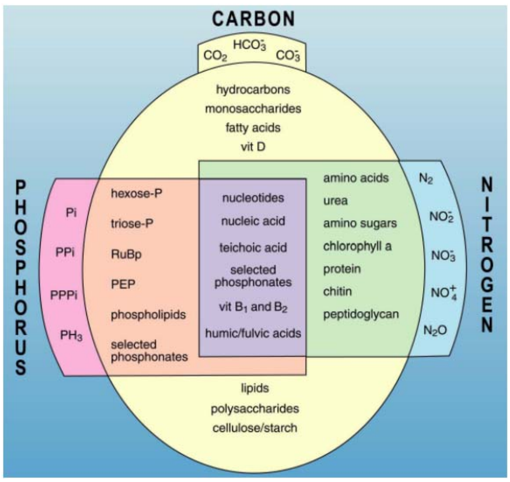

outline of this presentation

C, N P and Si reservoirs in the oceans

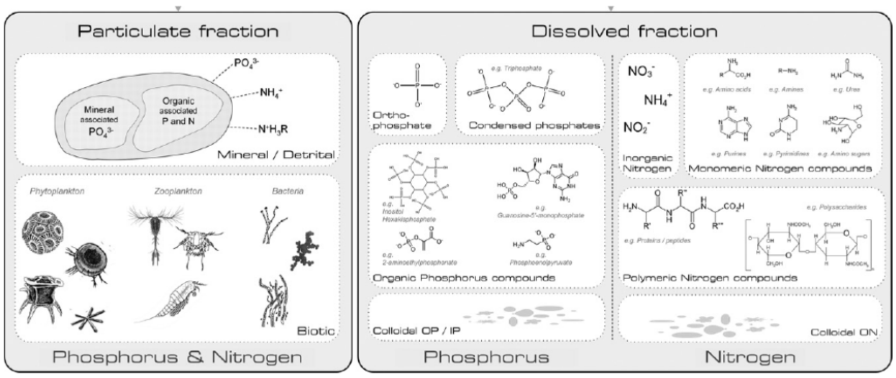

Fig. 2 – Representation of typical P and N components in the operationally defined dissolved and particulate fractions of a total sample.

Worsfold et al., Anal. Chim. Acta, 2008

outline of this presentation

dissolved inorganic compounds in the oceans

- dissolved inorganic nitrogen in the oceans
- dissolved inorganic phosphorus in the oceans
- dissolved silicon in the oceans

inorganic micro-nutrients in the oceans

dissolved inorganic nitrogen (DIN)

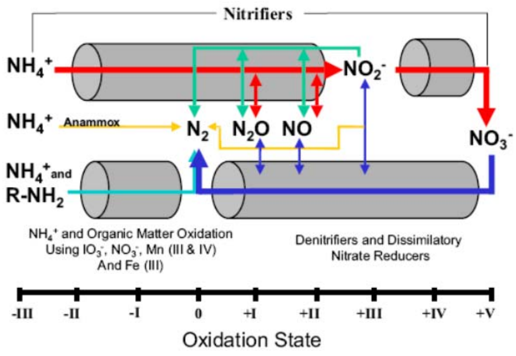

Fig. 1. This figure is re-drawn and updated from Codispoti et al. (2005). The suite of reactions supporting canonical denitrification are shown by the red (nitrification) and dark blue (canonical denitrification) arrows. The green arrows indicate a denitrification process that is associated with nitrification. This process produces N_2O and might also produce N_2. During these three processes, the intermediates, N_2O, NO, and NO_2^- can leave the cell and be changed between nitrifiers and denitrifiers. The NO_2^- produced can also support the anammox pathway (yellow arrows) in which NH_4^+ is oxidized to N_2 and NO_2^- is reduced to N_2. A review of the literature also suggests that oxidation of organic-N or NH_4^+ by NO_3^-, iodate (IO_3^-), oxidized metals such as Mn (III&IV), Fe (III) and various oxidized trace metals can also produce N_2 (light blue arrow). Not shown is the possibility that the oxidation of Mn (II) by NO_3^- may also produce N_2 (Luther et al., 1997). Intermediate chemicals involved in the anammox reaction (e.g. hydrazine) are omitted for simplicity.

dissolved inorganic nitrogen species

Codispoti, Biogeosciences, 2007

inorganic micro-nutrients in the oceans

dissolved inorganic nitrogen (DIN)

$$NO_3H \xrightarrow{k_{NO3}} NO_3^- + H^+$$

$$NO_2H \overset{k_{NO2}}{\Leftrightarrow} NO_2^- + H^+$$

$$NH_4^+ \overset{k_{NH4}}{\Leftrightarrow} NH_3\,(aq) + H^+$$

STANDARD SEAWATER

$K_{NO3}(35, 15) = 10^{2.3}$
$K_{NO2}(35,15) = 10^{-3.3}$
$K_{NH4}(35,15) = 10^{-9.68}$

pHsws= 8.0

NO_3^-/NO_3H	100% / 0%
NO_2^-/NO_2H	100% / 0%
NH_4^+/NH_3	98% / 2%

dissolved inorganic nitrogen species

inorganic micro-nutrients in the oceans

dissolved inorganic nitrogen (DIN)

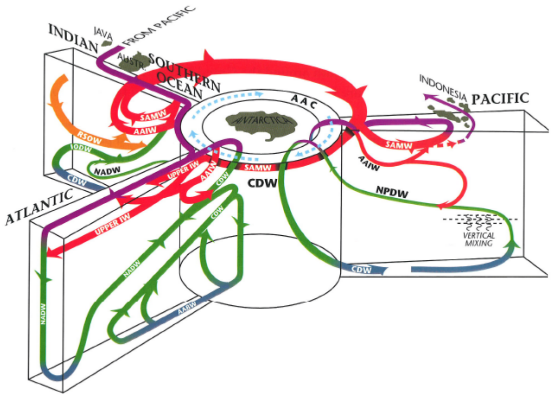

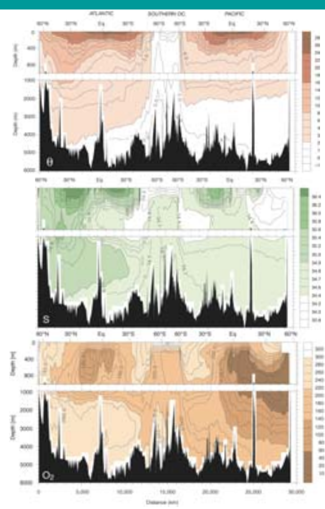

distribution of NO_3^- in the oceans

Schmitz, WHOI, 1995 Sarmiento & Gruber, 2006 (http://www.up.ethz.ch/people/ngruber/publications/textbook)

inorganic micro-nutrients in the oceans

dissolved inorganic nitrogen (DIN)

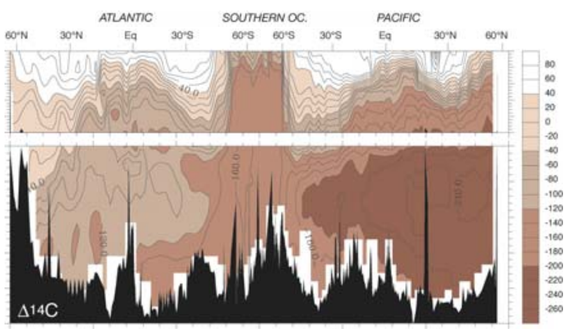

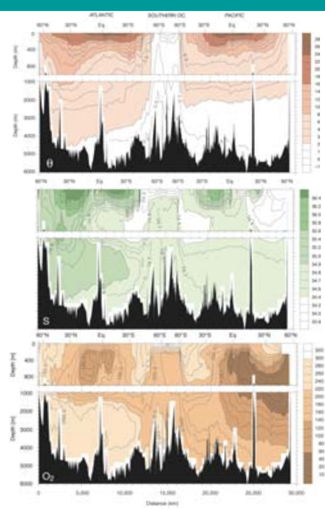

distribution of NO_3^- in the oceans

Sarmiento & Gruber, 2006 (http://www.up.ethz.ch/people/ngruber/publications/textbook)

inorganic micro-nutrients in the oceans

dissolved inorganic nitrogen (DIN)

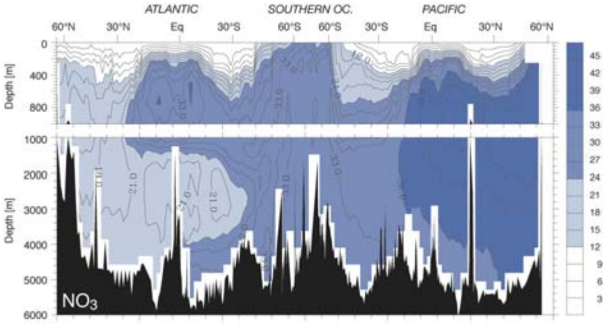

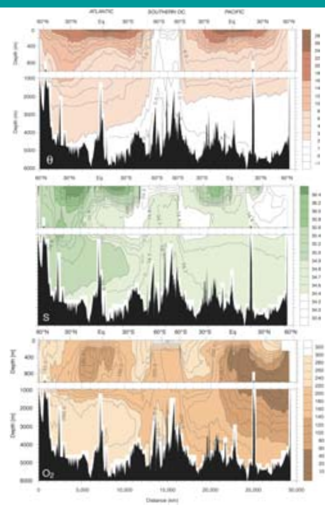

distribution of NO_3^- in the oceans

Sarmiento & Gruber, 2006 (http://www.up.ethz.ch/people/ngruber/publications/textbook)

inorganic micro-nutrients in the oceans

dissolved inorganic nitrogen (DIN)

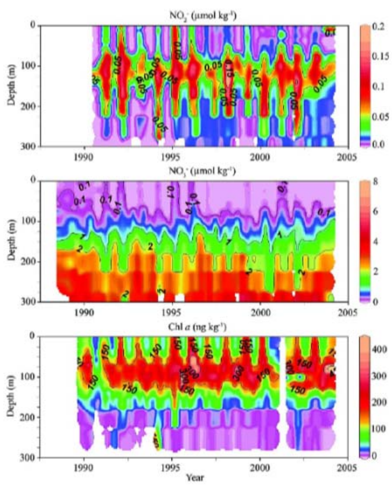

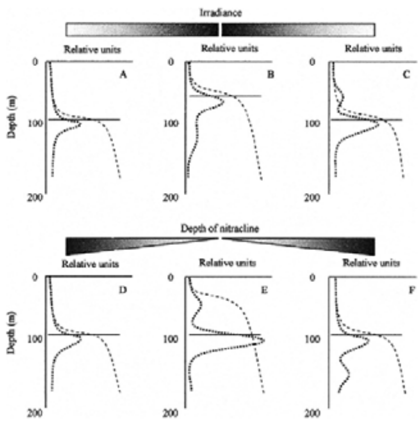

Fig. 3. Conceptual models of relative changes in the depth of 1% PAR (mean 93 m based on Siegel et al. 1997; solid line), nitracline (dashed line), and the primary nitrite maximum (dotted line) under the scenarios described in the text. Panels A–C represent a transition from periods of high to lower incident PAR (A→B) and back again (B→C). Panels D–F represent the vertical uplifting of the nitracline (due to an internal wave or eddy heaving; D→E) and subsequent relaxation (E→F). These models are described further in the text.

distribution of NO_2^- in the oceans: the primary maximum (< 1 µmol/kg)

Lomas & Lipschultz, Limnol. Oceanogr., 2006

inorganic micro-nutrients in the oceans
dissolved inorganic nitrogen (DIN)

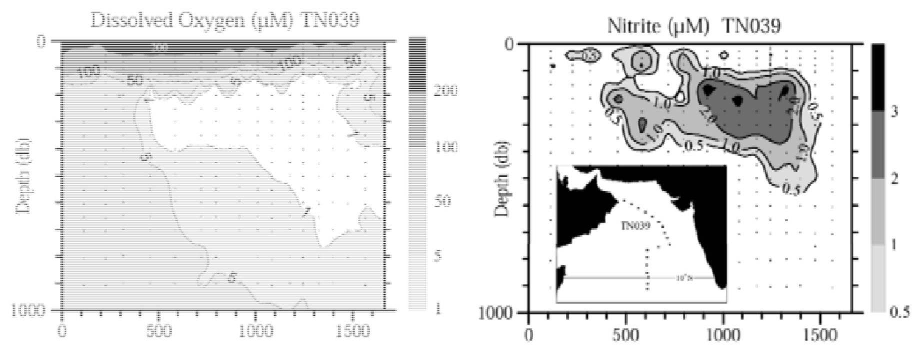

distribution of NO_2^- in the oceans: the secondary maximum (1-10 µmol/kg)

Codispoti et al., Sci. Mar., 2001

inorganic micro-nutrients in the oceans
dissolved inorganic nitrogen (DIN)

Se muestra seguidamente en cuatro ventanas las variables densidad, nitrógeno orgánico particulado, nitrato y amonio, a lo largo de una sección transversal de la Ría de Arousa.

En el centro de la imagen se incluye un indicador de las condiciones de afloramiento/hundimiento originadas por el arrastre del viento en plataforma. En condiciones de afloramiento una barra de color azul indicará la intensidad del mismo hasta valores de 3000 $m^3s^{-1}km^{-1}$ de costa. En condiciones de hundimiento una barra de color rojo se extiende hacia abajo hasta valores de 3000 $m^3s^{-1}km^{-1}$.

Las imágenes son resultado de la interpolación de datos reales obtenidos en muestreos realizados los lunes y los jueves de cada semana desde el 15 de mayo a 30 de octubre de 1989.

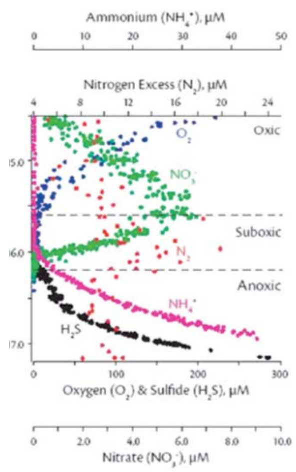

distribution of NH_4^+ in the oceans

inorganic micro-nutrients in the oceans
dissolved inorganic nitrogen (DIN)

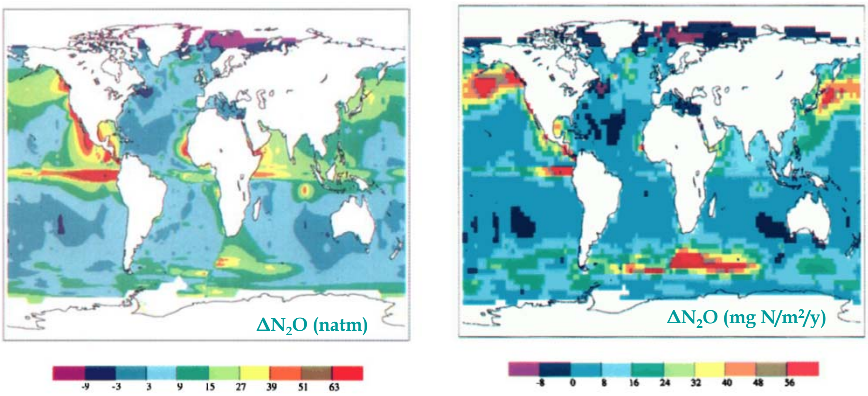

distribution of N_2O in the oceans

Nevison et al., Global Biogeochem. Cycles, 1995

inorganic micro-nutrients in the oceans
dissolved inorganic nitrogen (DIN)

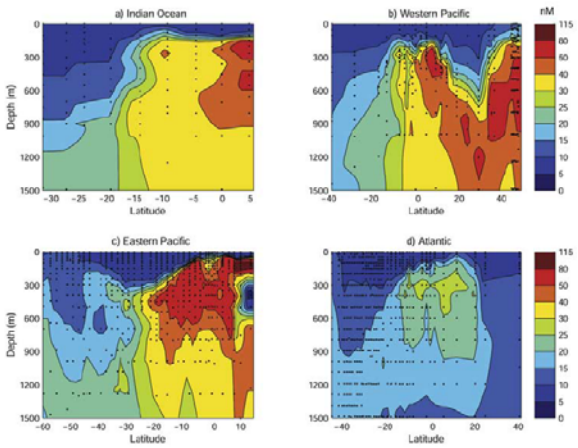

distribution of N_2O in the oceans

Nevison et al., Global Biogeochem. Cycles, 2003

inorganic micro-nutrients in the oceans

dissolved inorganic phosphorus (DIP)

K_{1P}

$H_3PO_4 \Leftrightarrow H_2PO_4^- + H^+$

K_{2P}

$H_2PO_4^- \Leftrightarrow HPO_4^{2-} + H^+$

K_{3P}

$HPO_4^{2-} \Leftrightarrow PO_4^{3-} + H^+$

STANDARD SEAWATER

$K_{1P}(35, 15) = 10^{-1.60}$

$K_{2P}(35,15) = 10^{-6.03}$

$K_{2P}(35,15) = 10^{-8.99}$

pHsws= 8.0

H_3PO_4	0.0%
$H_2PO_4^-$	0.8%
HPO_4^{2-}	88.4%
PO_4^{3-}	10.8%

dissolved inorganic phosphorus species

inorganic micro-nutrients in the oceans

dissolved inorganic phosphorus (DIP)

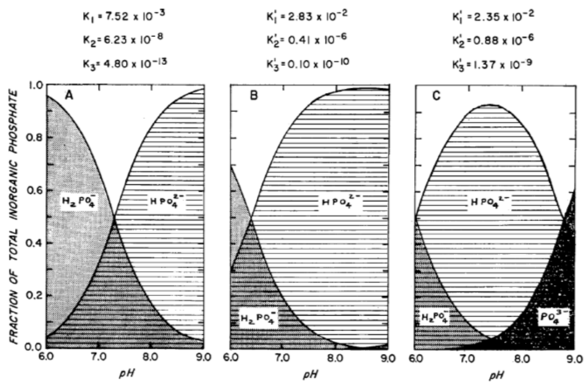

Fig. 3. Distribution of phosphate species at 20C. A. Pure water. B. 0.68 M NaCl. C. Artificial seawater, 33‰ salinity.

$MgH_2PO_4^+$, $CaH_2PO_4^+$, $MgHPO_4$, $CaHPO_4$, $MgPO_4^-$, $CaPO_4^-$

dissolved inorganic phosphorus species

Kester and . Pytkowicz, Linmol Oceanogr, 1967

inorganic micro-nutrients in the oceans

dissolved inorganic phosphorus (DIP)

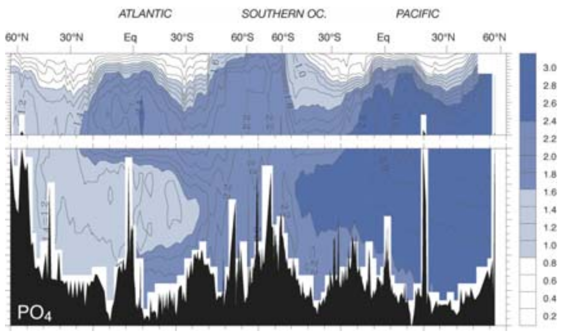

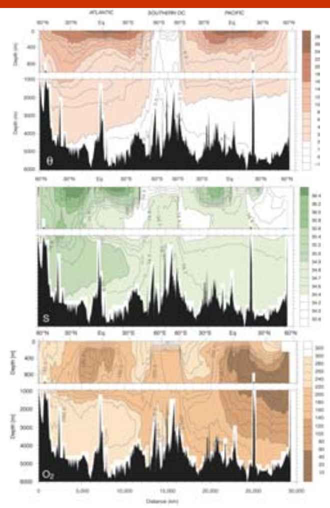

distribution of dissolved inorganic phsophorus in the oceans

Sarmiento & Gruber, 2006 (http://www.up.ethz.ch/people/ngruber/publications/textbook)

inorganic micro-nutrients in the oceans

dissolved silicon (SiO_2)

$$H_4SiO_4 \overset{K_{si}}{\Leftrightarrow} Si(OH)_3O^- + H^+$$

STANDARD SEAWATER

$K_{Si}(35,15) = 10^{-9.52}$

pHsws = 8.0

H_4SiO_4	96.7%
$Si(OH)_3O^-$	4.2%

dissolved inorganic silicon species

inorganic micro-nutrients in the oceans

dissolved silicon (SiO_2)

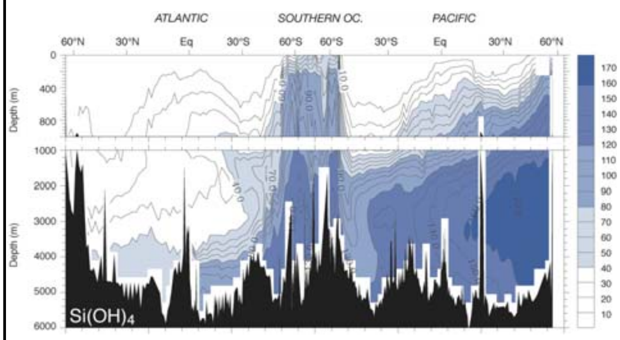

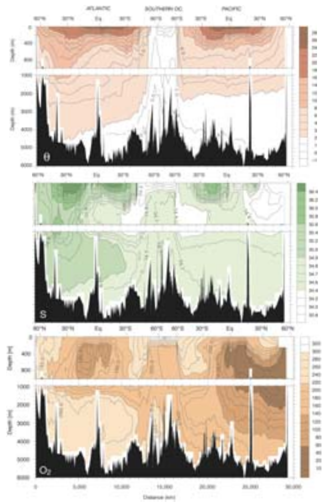

distribution of $Si(OH)_4$ in the oceans

Sarmiento & Gruber, 2006 (http://www.up.ethz.ch/people/ngruber/publications/textbook)

Impact of global change on ocean biogeochemical cycles (N, P, C and trace elements)
Palma de Mallorca, 4 – 8 Nov 2013

II. Biogenic materials in the oceans

X. Antón Álvarez Salgado

CSIC, Instituto de Investigacións Mariñas
C/ Eduardo Cabello 6, 36208 - Vigo
http://www.iim.csic.es

outline of this presentation

organic and inorganic biogenic compounds in the oceans

- **Biogenic inorganic compounds: silica and calcium carbonate**
- **Biogenic organic compounds: particulate organic matter**
- **Biogenic organic compounds: dissolved organic matter**

biogenic inorganic compounds
$SiO_2 \cdot n\,H_2O$

diatom

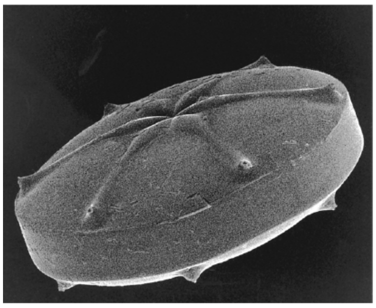

silicoflagelate

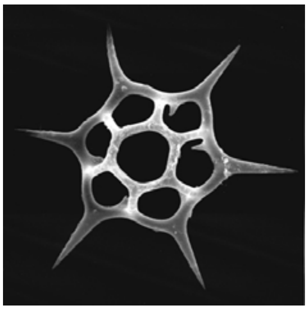

radiolaria

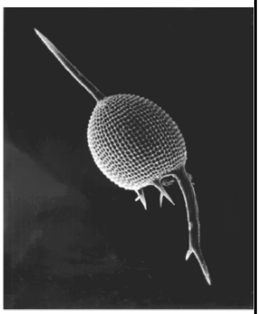

microorganisms with biogenic silica structures

biogenic inorganic compounds
$SiO_2 \cdot n\,H_2O$

$2\ Si(OH)_4 \rightarrow$
$\rightarrow (OH)_3Si\text{-}O\text{-}Si(OH)_3 +$
$+\ H_2O$

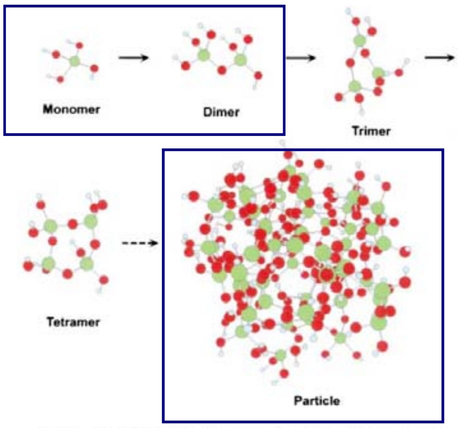

Figure 1. Polymerization behavior of silica. In aqueous solution monosilicic acid condenses to form dimeric, trimeric, and tetrameric (likely cyclic) structures, which then evolve to form particles with sizes in the nanometre range.

$SiO_2 \cdot n\,H_2O$ (~10% H_2O)

Insat. : 0.1% - 10%

polimerization of silicic acid

Coradin et al., Chem. Biochem., 2003

biogenic inorganic compounds

$SiO_2 \cdot n\,H_2O$

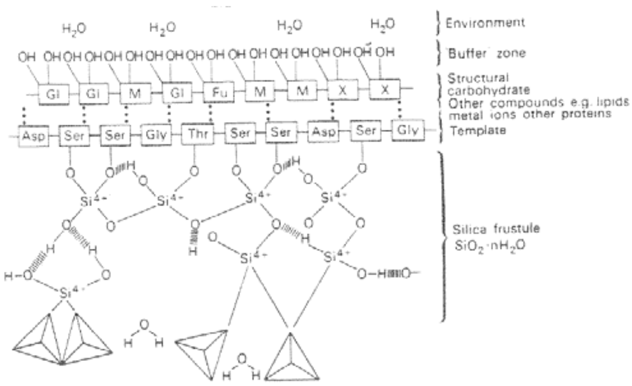

Fig. 4.7. Model of arrangement of layers in the cell wall of diatoms. Layer of polysaccharides with Gl (glucose), M (mannose), Fu (fucose) and X (xylose). Layer of template protein for polycondensation of $Si(OH)_4$ with Ser (serine), Thr (threonine), Asp (aspartic acid) and Gly (glycine). From Hecky *et al.* (1973).

Hecky et al., 1973

biogenic inorganic compounds

$SiO_2 \cdot n\,H_2O$

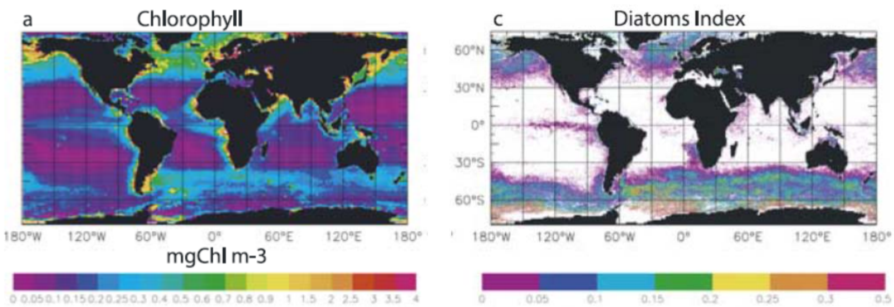

distribution of biogenic silica in the oceans

Bopp et al., Geophys. Res. Lett., 2005

biogenic inorganic compounds
$SiO_2 \cdot n\ H_2O$

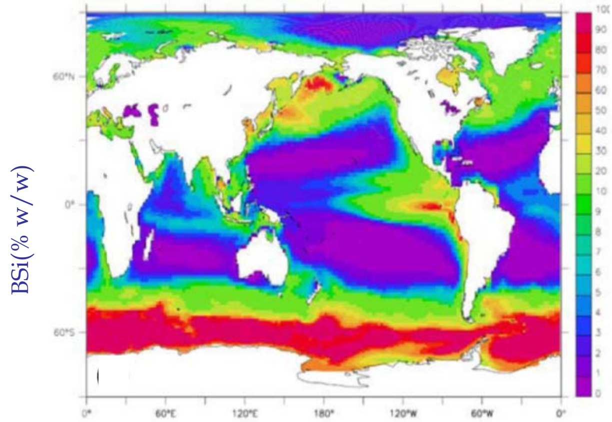

distribution of biogenic silica in marine sediments

Helhen et al., Biogeosciences, 2008

biogenic inorganic compounds
$CaCO_3$

coccolithophores

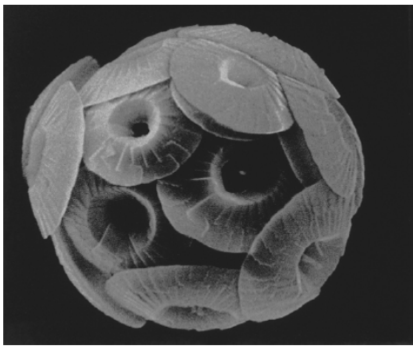

foraminiphers

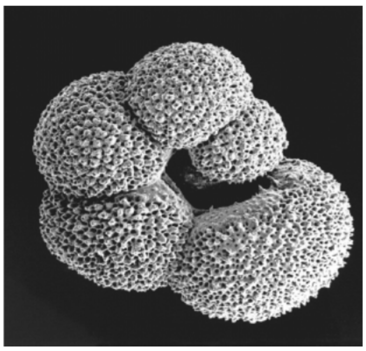

microorganisms with calcium carbonate structures

biogenic inorganic compounds
$CaCO_3$

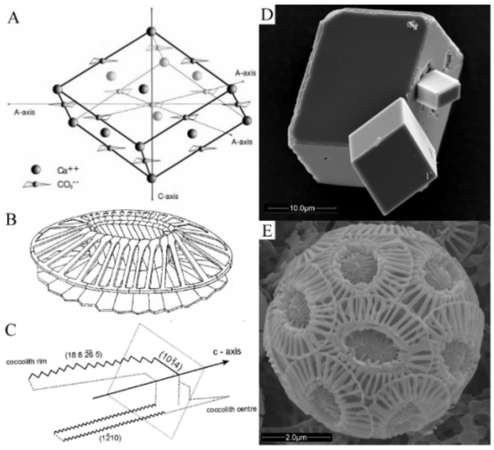

A) Sketch of a three dimensional array of a very small portion of $CaCO_3$ atoms in their spatial arrangement in calcite; reproduced from Young et al. (1999).
B) Drawing of a coccolith of *Emiliania huxleyi*; reproduced from Young et al. (1999)
C) Schematic cross-section through an *E. huxleyi* crystal showing its crystallographic relation to the calcite rhomb (grey); reproduced from Henriksen et al. (2004a).
D) SEM image of inorganically precipitated calcite (courtesy of Gernot Nehrke, AWIBremerhaven)
E) SEM image of *E. huxleyi*

Sobresat.: 250-400%

structure of a calcium carbonate cocolite

Langer, PhD Thesis, 2005

biogenic inorganic compounds
$CaCO_3$

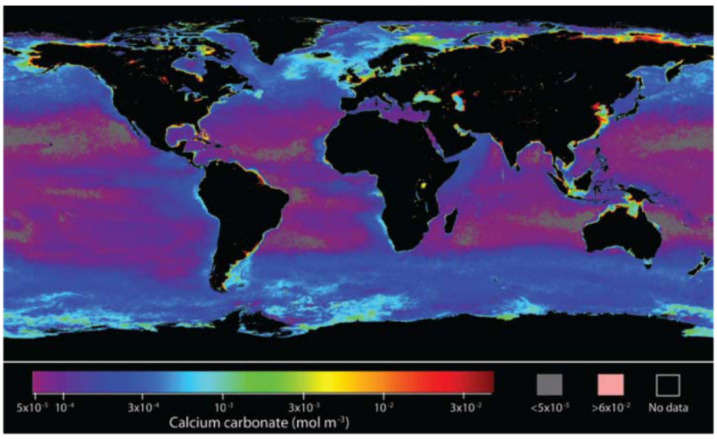

Figure 6. Merged two-band/three-band particulate inorganic carbon (PIC) algorithm showing coccolith PIC concentrations for the global ocean, averaged over the entire MODIS Aqua mission (January 1, 2002, to February 29, 2008). Color bar for PIC concentration (in mol PIC m^{-3}) shown at lower left. *Image produced by the NASA Ocean Color Group at the Goddard Space Flight Center*

distribution of $CaCO_3$ in the oceans

Balch & Utgoff, Oceanography, 2009

biogenic inorganic compounds
$CaCO_3$

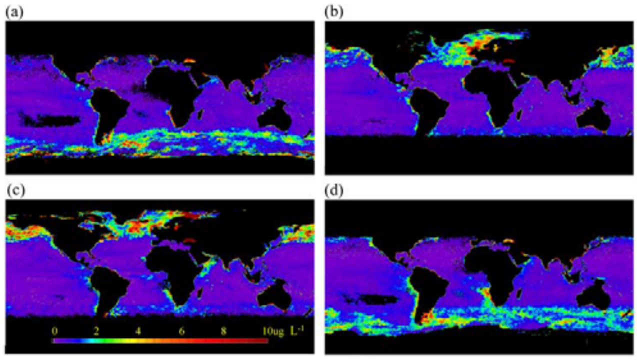

Figure 5. Global composite images of suspended PIC concentration calculated from MODIS/Terra data using two-band calcite algorithm. See text for other details of how the data were processed. The color scale is highlighted in Figure 5c. These data were binned into 36 km and 90 day averages, and thus the standard error will be <0.08 μgPIC L^{-1} (see Table 2), well below the average seawater concentration of ~2 μgPIC L^{-1}. (a) January–March. (b) April–June. (c) July–September. (d) October–December.

distribution of $CaCO_3$ in the oceans

Balch et al., Global Bigeochem. Cy., 2005

biogenic inorganic compounds
$CaCO_3$

$CaCO_3$ (% w/w)

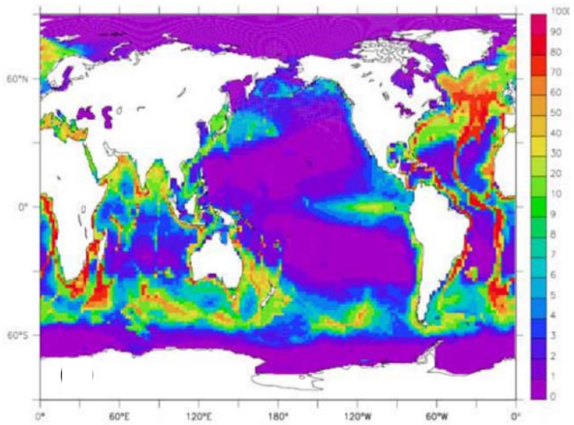

distribution of $CaCO_3$ in marine sediments

Helhen et al., Biogeosciences, 2008

biogenic organic compounds

particulate organic matter (POM)

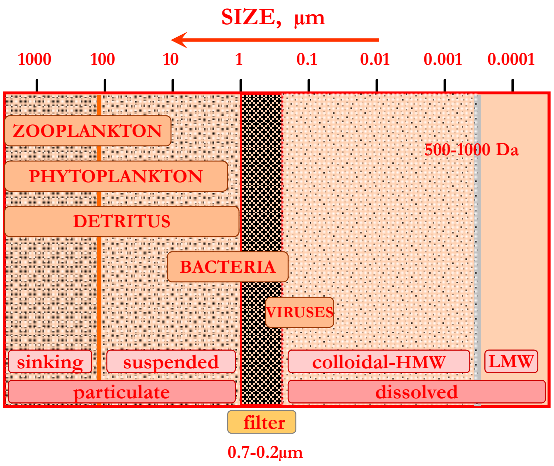

DOM	662	Gt−C
detritus	20	Gt−C
phytoplankton	1−3	Gt−C
zooplankton	0.1	Gt−C
bacteria	0.1	Gt−C

partition of organic matter in the oceans

Gould & Mantoura (1990)

biogenic organic compounds

particulate organic matter (POM)

	fórmula	m.w	% (w/w)
Carbohydrates	$C_6H_{10}O_5$	456,4	24,4
Lipids	$C_{53}H_{89}O_6$	822,3	16,5
Pigments	$C_{46}H_{52}O_5N_4Mg$	764,3	2,0
Proteins	$C_{139}H_{217}O_{45}N_{39}S$	3171,0	45,1
Phosphorus comp.	$C_{45}H_{76}O_{31}N_{12}P_5$	1436,0	12,0
Avg. composition	$\mathbf{C_{106}H_{171}O_{44}N_{16}PS_{0.3}}$		**100,0**

POM composition and contribution to alkalinity

Fraga & Álvarez-Salgado, Ciencias Marina, 2006

biogenic organic compounds

particulate organic matter (POM)

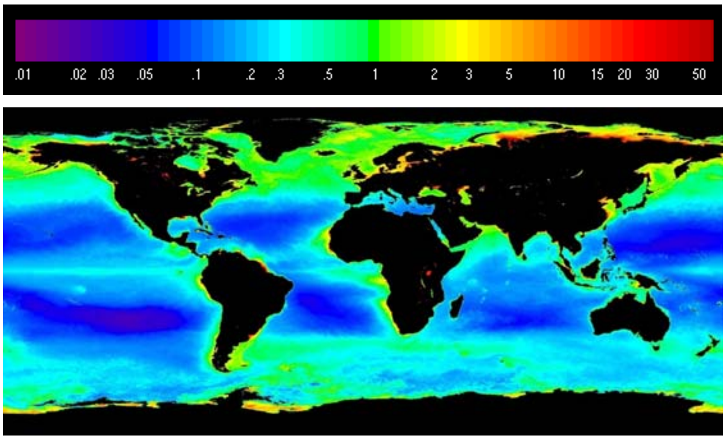

distribution of POM in the oceans

biogenic organic compounds

particulate organic matter (POM)

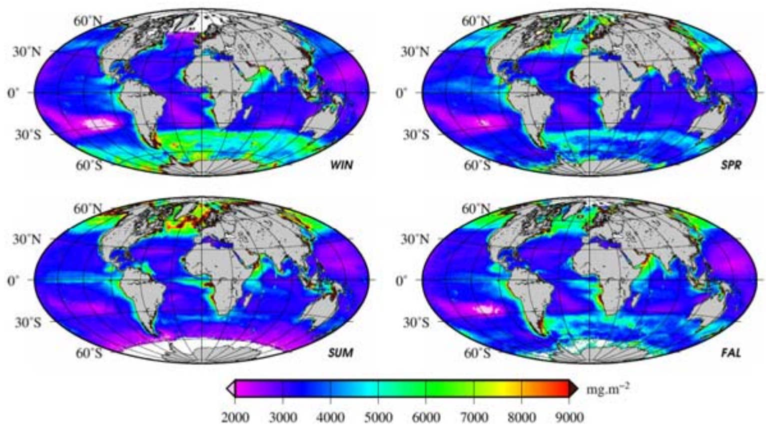

Fig. 11. Same as Fig. 10 but for the integrated content of POC over the euphotic layer.

distribution of POM in the oceans

Duforet-Gaurnier et al., Deep Sea Res., 2010

biogenic organic compounds

particulate organic matter (POM)

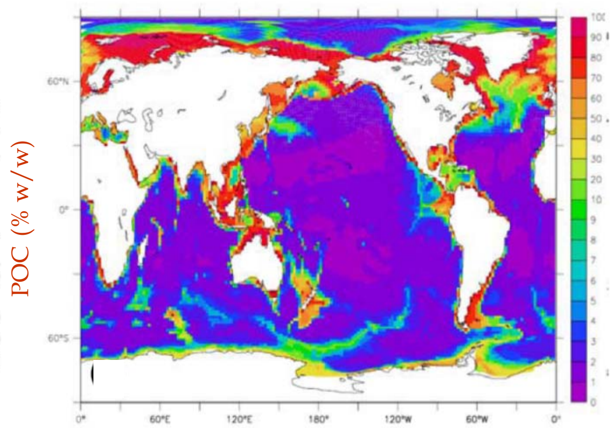

distribution of POM in marine sediments

Helhen et al., Biogeosciences, 2008

biogenic organic compounds

dissolved organic matter (DOM)

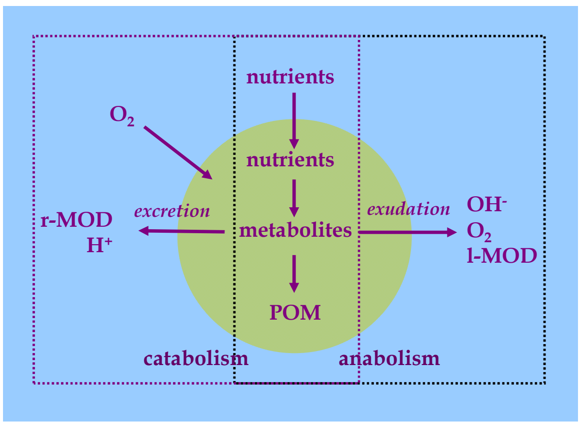

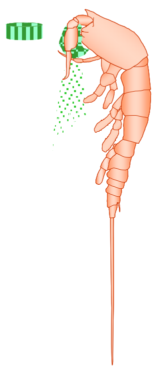

Mesozoo lysis

origin of dissolved organic matter: <u>biotic</u>

Brook, Nature, 2008

biogenic organic compounds

dissolved organic matter (DOM)

melanoidins

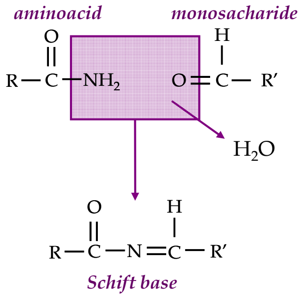

poly-insaturate fattly acids

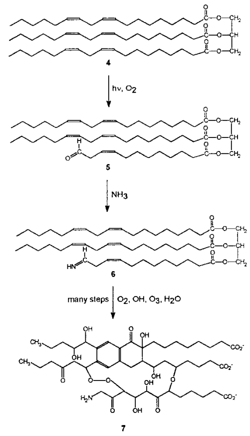

origin of dissolved organic matter: abiotic

biogenic organic compounds

dissolved organic matter (DOM)

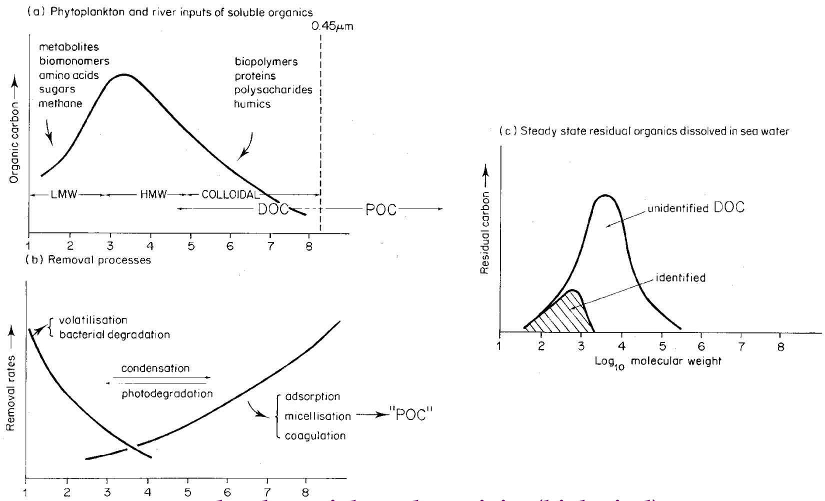

molecular weight and reactivity (biological)

Jickells et al., 1991

biogenic organic compounds
dissolved organic matter (DOM)

DOM		contribution	τ (days)	fate
labile	l-MOD	< 5%	10^{-2}–10^{1}	recycling
semi–labile	s-MOD	< 20%	10^{2}	export
refractory	r-MOD	> 75%	10^{3}–10^{6}	inmovilisation

molecular weight and reactivity (biological)

biogenic organic compounds
dissolved organic matter (DOM)

	LMW–MOD	HMW–MOD
mol. weight	< 1 kDa	> 1 kDa
contribution	~70%	~30%
l–DOM	monosacharides, aminoacids, urea, fattly acids, glicolate	sugar polymers, amides, peptides, phosphoric esters, phosphonates
	(τ~ hours–days)	(τ~ days–weeks)
r–DOM	?	humic susbtances
	(τ~4000–6000 years)	(τ ~ 150–200 years)

molecular weight and reactivity (biological)

biogenic organic compounds
dissolved organic matter (DOM)

humic acid

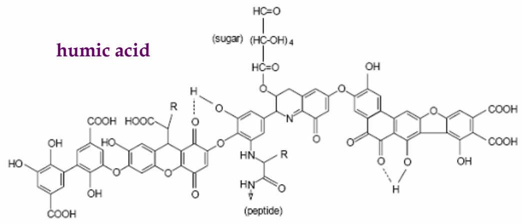

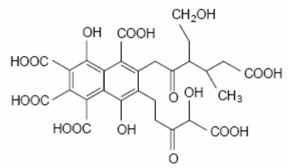

fulvic acid

humic substances

Ritchie & Perdue, Geochim. Cosmochim. Acta, 2003

biogenic organic compounds
dissolved organic matter (DOM)

fulvic acid		humic acid		humins
light yellow	dark yellow	brown	dark grey	black

color →

polymerization degree →

2000 — Molecular weight → 300.000

45% — Carbon content → 62%

48% — Oxygen content → 30%

insolubility in water →

humic substances

Stevenson, 1982

biogenic organic compounds
dissolved organic matter (DOM)

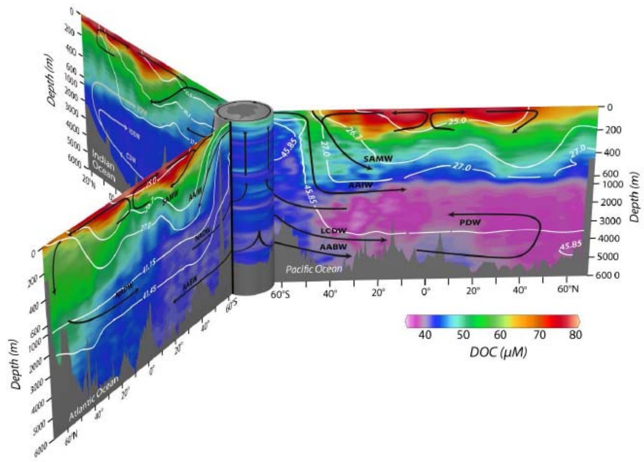

distribution of DOM in the oceans

Hansell et al., Oceanography, 2009

Impact of global change on ocean biogeochemical cycles (N, P, C and trace elements)
Palma de Mallorca, 4– 8 Nov 2013

III. Metabolism of the oceans: synthesis and mineralization processes

X. Antón Álvarez Salgado
CSIC, Instituto de Investigacións Mariñas
C/ Eduardo Cabello 6, 36208 - Vigo
http://www.iim.csic.es

outline of this presentation

anabolism and catabolism of the microbial communities

stoichiometry of metabolic processes in the microbial food web

- **synthesis of biogenic materials**
- **aerobic mineralisation of biogenic materials**
- **anaerobic mineralisation of biogenic materials**

synthesis of biogenic materials

synthesis of organic matter by marine phytoplankton

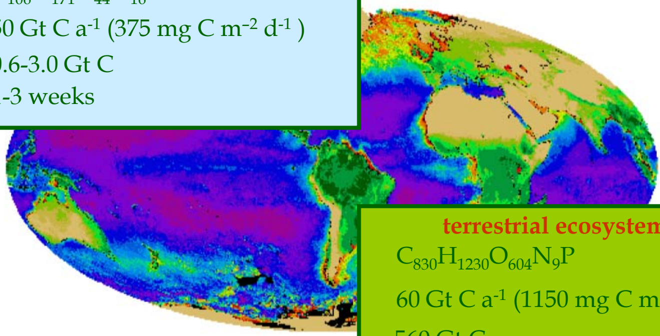

marine ecosystems

$C_{106}H_{171}O_{44}N_{16}P$

50 Gt C a^{-1} (375 mg C m^{-2} d^{-1})

0.6-3.0 Gt C

1-3 weeks

terrestrial ecosystem

$C_{830}H_{1230}O_{604}N_{9}P$

60 Gt C a^{-1} (1150 mg C m^{-2} d^{-1})

560 Gt C

10 years

global distribution of primary production

synthesis of biogenic materials

synthesis of organic matter by marine phytoplankton

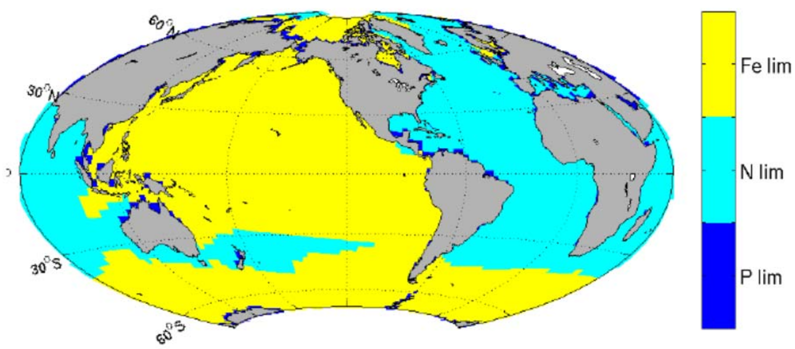

limiting elements of marine primary production

Bernard et al., Biogeosciences disc., 2009

synthesis of biogenic materials

synthesis of organic matter by marine phytoplankton

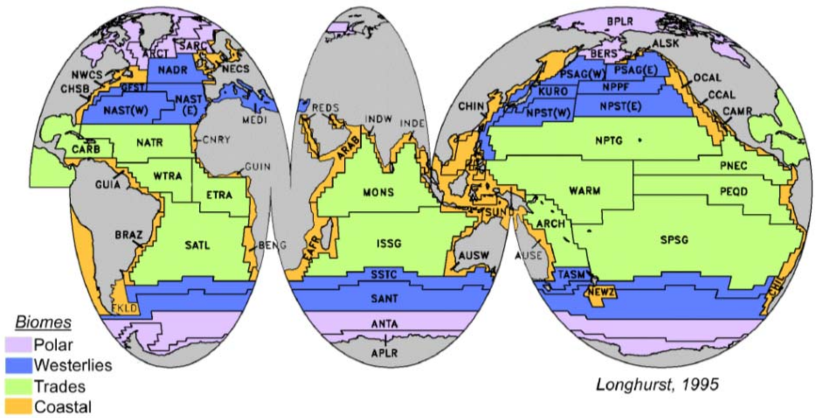

biogeographic provinces in the oceans

Longhurst, Progr. Oceanogr., 1995

synthesis of biogenic materials

synthesis of organic matter by marine phytoplankton

	formula	**% (w/w)**
Carbohydrates	$C_6H_{10}O_5$	24,4
Lipids	$C_{53}H_{89}O_6$	16,5
Chlorophyll a, b, c_1 y c_2	$C_{46}H_{52}O_5N_4Mg$	2,0
Proteins	$C_{139}H_{217}O_{45}N_{39}S$	45,1
Phosphorus compounds	$C_{45}H_{76}O_{31}N_{12}P_5$	12,0
Average composition	$C_{106}H_{171}O_{44}N_{16}PS_{0.3}$	**100,0**

composition of phytoplanktonic organic matter

Fraga & Álvarez-Salgado, Cienc. Mar., 2005

synthesis of biogenic materials

synthesis of organic matter by marine phytoplankton

$$CO_2 + H_2O \overset{K_1}{\Leftrightarrow} HCO_3^- + H^+$$

$$HCO_3^- \overset{K_2}{\Leftrightarrow} CO_3^{2-} + H^+$$

$$H_3BO_3 + H_2O \overset{K_B}{\Leftrightarrow} B(OH)_4^- + H^+$$

STANDARD SEAWATER

($pHsws = 8.0$; $\Sigma CO_2 = 2100\ \mu mol\ kg^{-1}$)

$K_1(35, 15) = 10^{-6.04}$	$[CO_2] = 13.8\ \mu mol\ kg^{-1}$ (0.7%)
$K_2(35,15) = 10^{-9.23}$	$[HCO_3^-] = 1916.5\ \mu mol\ kg^{-1}$ (91.3%)
$\alpha_S(35,15) = 10^{-1.43}$	$[CO_3^{2-}] = 169.6\ \mu mol\ kg^{-1}$ (8.0%)
$K_B(35, 15) = 10^{-8.74}$	$[B(OH)_4^-] = 88.7\ \mu mol\ kg^{-1}$ (21.3%)
	$[H_3BO_3] = 327.7\ \mu mol\ kg^{-1}$ (78.7%)

ΣCO_2 sources and buffering capacity of seawater

synthesis of biogenic materials

ΣCO_2 sources of marine phytoplankton photosynthesis

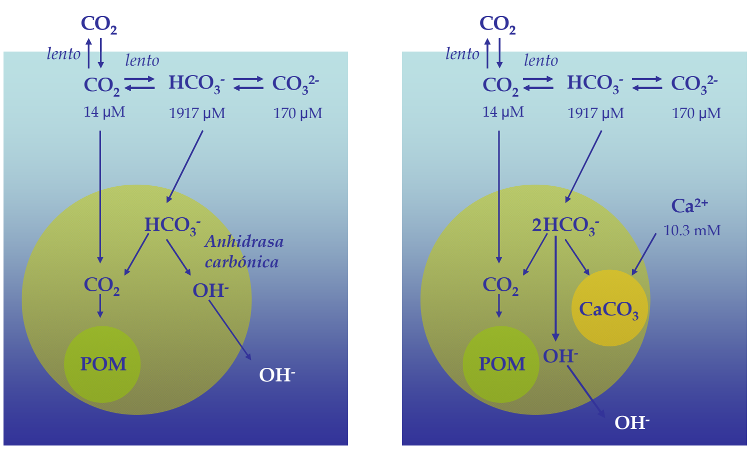

mechanisms of incorporation of CO_2 y HCO_3^-

De Baar, Prog. Oceanogr., 1994

synthesis of biogenic materials

using NH_4^+ as nitrogen source

$$106\ HCO_3^- + 16\ NH_4^+ + HPO_4^{2-} + 46\ H_2O \longrightarrow C_{106}H_{171}O_{44}N_{16}P + 116\ O_2 + 92\ OH^-$$

assuming no buffering capacity

	initial	ΔCorg = 106	final
pH	8.00	+1.40	9.40

stoichiometry of the synthesis of biogenic materials

synthesis of biogenic materials

using NH_4^+ as nitrogen source

assuming HCO_3^- / CO_3^{2-} buffer only:

$$106\ HCO_3^- + 16\ NH_4^+ + HPO_4^{2-} + 46\ H_2O \longrightarrow C_{106}H_{171}O_{44}N_{16}P + 116\ O_2 + 92\ OH^-$$

+

$$HCO_3^- + OH^- \Leftrightarrow CO_3^{2-} + H_2O$$

$$198\ HCO_3^- + 16\ NH_4^+ + HPO_4^{2-} \longrightarrow C_{106}H_{171}O_{44}N_{16}P + 116\ O_2 + 92\ CO_3^{2-} + 46\ H_2O$$

$$pH = -\log_{10}(K_2 \cdot f_H) + \log_{10}\left(\frac{[CO_3^{2-}]}{[HCO_3^-]}\right)$$

	initial	ΔCorg= 106	final
pH	8.00	+0.23	8.23

buffering capacity of seawater

synthesis of biogenic materials

using NH_4^+ as nitrogen source

seawater pH buffer:

variable	initial	ΔCorg= 106	final
$\sum CO_2$ (μmol·kg^{-1})	2100	-106	1994
A (μmol·kg^{-1})	2348	-16	2332
pH	8.00	+0.16	8.16
$[CO_2]$ (μmol·kg^{-1})	13.8	-5.0	8.8
$[HCO_3^-]$ (μmol·kg^{-1})	1917	-157	1760
$[CO_3^{2-}]$ (μmol·kg^{-1})	170	+55	225
Ω_{ARG}	2.6		3.5
Ω_{CAL}	4.1		5.3
$pCO_2(g)$ (μatm)	370	-135	235
$[O_2]$ (μmol·kg^{-1})	248	+116	364

stoichimetry and buffering capacity

synthesis of biogenic materials

using NO_3^- as nitrogen source

$NO_3^- \longrightarrow NO_2^- + 1/2\, O_2$ *(nitrate reductase)*

$NO_2^- + 3\, H_2O \longrightarrow NH_4^+ + 3/2\, O_2 + 2\, OH^-$ *(nitrite reductase)*

assimilative reduction

+

$$106\, HCO_3^- + 16\, NH_4^+ + HPO_4^{2-} + 46\, H_2O \longrightarrow C_{106}H_{171}O_{44}N_{16}P + 116\, O_2 + 92\, OH^-$$

$$106\, HCO_3^- + 16\, NO_3^- + HPO_4^{2-} + 94\, H_2O \longrightarrow C_{106}H_{171}O_{44}N_{16}P + 148\, O_2 + 124\, OH^-$$

+

$$HCO_3^- + OH^- \Leftrightarrow CO_3^{2-} + H_2O$$

$$230\, HCO_3^- + 16\, NO_3^- + HPO_4^{2-} \longrightarrow C_{106}H_{171}O_{44}N_{16}P + 148\, O_2 + 124\, CO_3^{2-} + 30\, H_2O$$

stoichiometry of the synthesis of biogenic materials

synthesis of biogenic materials

using NO_3^- as nitrogen source

variable	initial	ΔCorg= 106	final
$\sum CO_2$ (µmol ·kg^{-1})	2100	+106	1994
A (µmol ·kg^{-1})	2348	+16	2364
pH	8.00	+0.21	8.21
[CO_2] (µmol ·kg^{-1})	13.8	-6.1	7.7
[HCO_3^-] (µmol ·kg^{-1})	1917	-180	1734
[CO_3^{2-}] (µmol ·kg^{-1})	170	+80	249
Ω_{ARG}	2.6		3.8
Ω_{CAL}	4.1		6.0
$p$$CO_2$(g) (µatm)	370	-163	207
[O_2] (µmol ·kg^{-1})	248	+148	396

stoichiometry and buffering capacity

synthesis of biogenic materials

using N_2 as nitrogen source

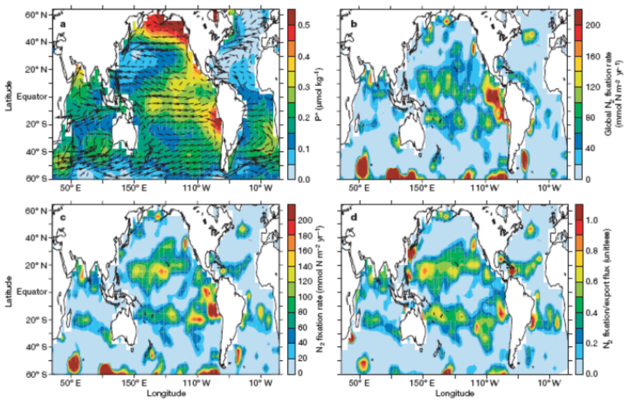

Figure 2 | Annual mean distribution of P*, ocean currents, and the N_2 fixation rates determined from them at 0–120 m depth. **a**, The P* distribution ($P^* = PO_4^{3-} - NO_3^-/r_n$) is based on climatological data from the World Ocean Atlas[30], and the surface velocity is computed from the MOM3 ocean general circulation model[30]. **b**, Global N_2 fixation rates diagnosed from the convergence of excess inorganic PO_4^{3-}, $-\lambda\nabla\cdot\Phi(P^*)$, which requires an excess uptake of PO_4^{3-} relative to the biological N requirement. **c**, Rates of N_2 fixation accounting for both inorganic and organic nutrient pools, equal to $-\lambda\nabla\cdot\Phi(P_t^*)$ where this term is positive (that is, where excess P_t converges). **d**, N_2 fixation rates (from **c**) as a fraction of the export flux of organic matter.

global distribution of N_2 fixation in the oceans

Deutsch et al., Nature, 2007

synthesis of biogenic materials

using N_2 as nitrogen source

$N_2\uparrow + 5\,H_2O \longrightarrow 2\,NH_4^+ + 3/2\,O_2 + 2\,OH^-$ *(nitrogenase) – Trichodesmiun & cianobacteria*

\+ $106\,HCO_3^- + 16\,NH_4^+ + HPO_4^{2-} + 46\,H_2O \longrightarrow C_{106}H_{171}O_{44}N_{16}P + 116\,O_2 + 92\,OH^-$

$106\,HCO_3^- + 8\,N_2\uparrow + HPO_4^{2-} + 86\,H_2O \longrightarrow C_{106}H_{171}O_{44}N_{16}P + 128\,O_2 + 108\,OH^-$

\+ $HCO_3^- + OH^- \Leftrightarrow CO_3^{2-} + H_2O$

$214\,HCO_3^- + 8\,N_2\uparrow + HPO_4^{2-} \longrightarrow C_{106}H_{171}O_{44}N_{16}P + 128\,O_2 + 108\,CO_3^{2-} + 22\,H_2O$

stoichiometry of the synthesis of biogenic materials

synthesis of biogenic materials

using N_2 as nitrogen source

variable	initial	ΔCorg= 106	final
$\sum CO_2$ (µmol·kg^{-1})	2100	-106	1994
A (µmol·kg^{-1})	2348	+0	2348
pH	8.00	+0.18	8.18
$[CO_2]$ (µmol·kg^{-1})	13.8	-5.5	8.3
$[HCO_3^-]$ (µmol·kg^{-1})	1917	-167	1750
$[CO_3^{2-}]$ (µmol·kg^{-1})	170	+66	236
Ω_{ARG}	2.6		3.6
Ω_{CAL}	4.1		5.7
pCO$_2$(g) (µatm)	370	-149	221
$[O_2]$ (µmol·kg^{-1})	248	+128	376

stoichiometry and buffering capacity

synthesis of biogenic materials

using multiple nitrogen sources

$$198\,HCO_3^- + 16\,NH_4^+ + HPO_4^{2-} \longrightarrow C_{106}H_{171}O_{44}N_{16}P + 116\,O_2 + 92\,CO_3^{2-} + 46\,H_2O$$

$$230\,HCO_3^- + 16\,NO_3^- + HPO_4^{2-} \longrightarrow C_{106}H_{171}O_{44}N_{16}P + 148\,O_2 + 124\,CO_3^{2-} + 30\,H_2O$$

$$214\,HCO_3^- + 8\,N_2\uparrow + HPO_4^{2-} \longrightarrow C_{106}H_{171}O_{44}N_{16}P + 128\,O_2 + 108\,CO_3^{2-} + 22\,H_2O$$

stoichiometry of the synthesis of biogenic materials

synthesis of biogenic materials

using multiple nitrogen sources

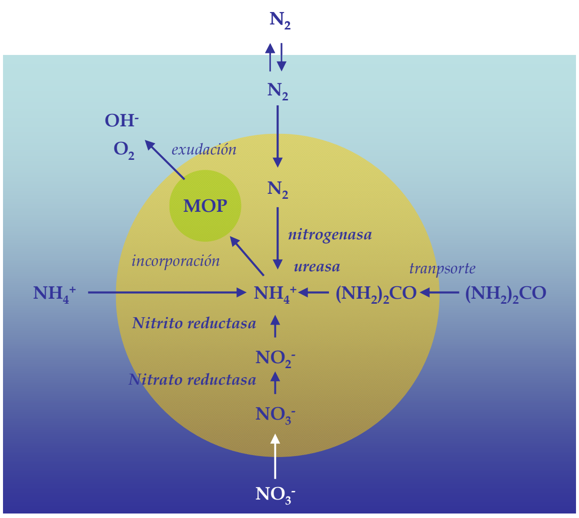

synthesis of biogenic materials

synthesis of calcium carbonate in the oceans

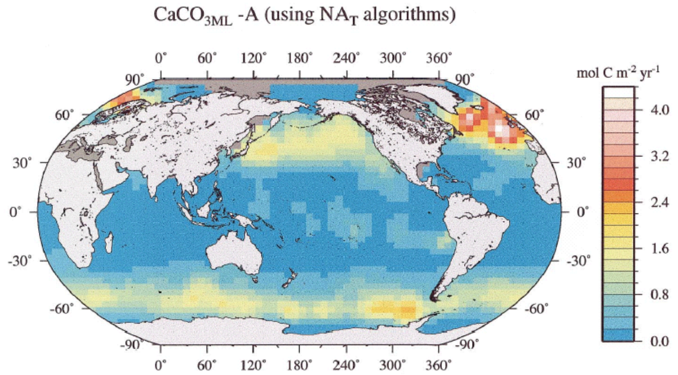

Fig. 4. Annual rate of net $CaCO_3$ production integrated from the surface to the base of the mixed layer as derived from the magnitude of seasonal NA_{POT} decrease calculated from regional NA_T/SST algorithms and seasonal mean SST and NO_3^- fields. Values are expressed as mole C m^{-2} yr^{-1}. Globally integrated net $CaCO_3$ production for 1990 is 1.1 Gt C yr^{-1}.

global distribution of calcification in the oceans: 1,1 ± 0,3 × 10^{15} g C/yr

Lee, 2001

synthesis of biogenic materials

synthesis of calcium carbonate in the oceans

$$CO_3^{2-} + Ca^{2+} \longrightarrow CaCO_3\,(s)$$ 50%

+

$$230\,HCO_3^- + 16\,NO_3^- + HPO_4^{2-} \longrightarrow C_{106}H_{171}O_{44}N_{16}P + 148\,O_2 + 124\,CO_3^{2-} + 30\,H_2O$$ 50%

$$230\,HCO_3^- + 16\,NO_3^- + HPO_4^{2-} + 106\,Ca^{2+} \longrightarrow (C_{106}H_{171}O_{44}N_{16}P)(CaCO_3)_{106} + 148\,O_2 + 18\,CO_3^{2-} + 30\,H_2O$$

stoichiometry of the synthesis of biogenic materials

synthesis of biogenic materials

synthesis of calcium carbonate in the oceans

ΔCorg = Δ $CaCO_3$, ΔN_T = Δ [NO_3^-] (cocolitofores using nitrate as nitrogen source)

Variable	inicial	ΔCorg= 106	final
$\sum CO_2$ (μmol·kg^{-1})	2100	-212	1888
A (μmol·kg^{-1})	2348	-196	2152
pH	8.00	+0.06	8.06
[CO_2] (μmol·kg^{-1})	13.8	-3.1	10.7
[HCO_3^-] (μmol·kg^{-1})	1917	-212	1704
[CO_3^{2-}] (μmol·kg^{-1})	170	4	173
Ω_{ARG}	2.6		2.7
Ω_{CAL}	4.1		4.2
$p$$CO_2$(g) (μatm)	370	-84	286
[O_2] (μmol·kg^{-1})	248	+148	396

stoichimetry and buffering capacity

synthesis of biogenic materials

synthesis of biogenic silica in the oceans

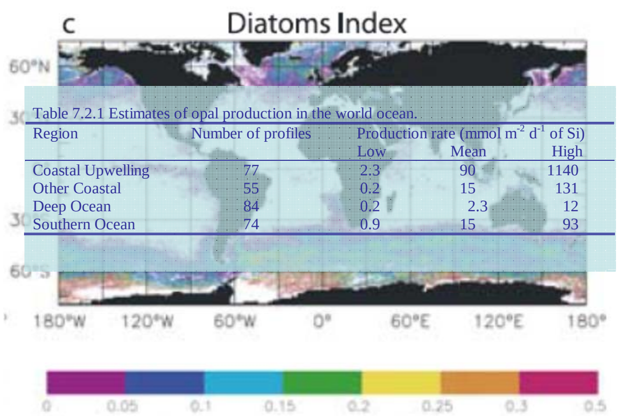

Table 7.2.1 Estimates of opal production in the world ocean.

Region	Number of profiles	Production rate (mmol m^{-2} d^{-1} of Si) Low	Mean	High
Coastal Upwelling	77	2.3	90	1140
Other Coastal	55	0.2	15	131
Deep Ocean	84	0.2	2.3	12
Southern Ocean	74	0.9	15	93

global distribution of silification in the oceans: 6,85 10^{15} g/yr

Bopp et al., Geophys. Res. Lett., 2005

synthesis of biogenic materials

synthesis of biogenic silica in the oceans

$$H_4SiO_4 + (n\text{-}2)\, H_2O \longrightarrow SiO_2 \cdot nH_2O_{(s)}$$

$+$

$$230\, HCO_3^- + 16\, NO_3^- + HPO_4^{2-} \longrightarrow C_{106}H_{171}O_{44}N_{16}P + 148\, O_2 + 124\, CO_3^{2-} + 30\, H_2O$$

$$230\, HCO_3^- + 16\, NO_3^- + HPO_4^{2-} + 16\, H_4SiO_4 \longrightarrow (C_{106}H_{171}O_{44}N_{16}P)(SiO_2 \cdot nH_2O)_{16} + 148\, O_2 + 18\, CO_3^{2-} + 30\, H_2O$$

stoichiometry of the synthesis of biogenic materials

synthesis of biogenic materials

synthesis of biogenic silica in the oceans

ΔNorg = $\Delta SiO_2 \cdot nH_2O$, $\Delta N_T = \Delta [NO_3^-]$ (disatoms using nitrate as nitrogen source)

variable	initial	ΔCorg= 106	final
ΣCO_2 (µmol kg^{-1})	2100	+106	1994
A (µmol kg^{-1})	2348	+16	2364
pH	8.00	+0.21	8.21
$[CO_2]$ (µmol kg^{-1})	13.8	-6.1	7.7
$[HCO_3^-]$ (µmol kg^{-1})	1917	-180	1734
$[CO_3^{2-}]$ (µmol kg^{-1})	170	+80	249
Ω_{ARG}	2.6		3.8
Ω_{CAL}	4.1		6.0
pCO_2(g) (µatm)	370	-163	207
$[O_2]$ (µmol kg^{-1})	248	+148	396

stoichiometry and buffering capacity

aerobic mineralization of biogenic materials

ammonification

$$C_{106}H_{171}O_{44}N_{16}P + 116\ O_2 + 46\ H_2O \longrightarrow 106\ HCO_3^- + 16\ NH_4^+ + HPO_4^{2-} + 92\ H^+$$

$+$

$$CO_3^{2-} + H^+ \Leftrightarrow HCO_3^-$$

$$C_{106}H_{171}O_{44}N_{16}P + 116\ O_2 + 92\ CO_3^{2-} + 46\ H_2O \longrightarrow 198\ HCO_3^- + 16\ NH_4^+ + HPO_4^{2-}$$

stoichiometry of the mineralization of biogenic materials

aerobic mineralization of biogenic materials

ammonification

variable	initial	ΔCorg=-106	final
$\sum CO_2$ (μmol·kg^{-1})	2100	+106	2206
A (μmol·kg^{-1})	2348	+16	2364
pH	8.00	-0.19	7.81
$[CO_2]$ (μmol·kg^{-1})	13.8	+9.4	23.3
$[HCO_3^-]$ (μmol·kg^{-1})	1917	+149	2065
$[CO_3^{2-}]$ (μmol·kg^{-1})	170	-52	117
Ω_{ARG}	2.6		1.8
Ω_{CAL}	4.1		2.8
$pCO_2(g)$ (μatm)	370	+252	621
$[O_2]$ (μmol·kg^{-1})	248	-116	132

stoichiometry and buffering capacity

aerobic mineralization of biogenic materials

nitrification

$$C_{106}H_{171}O_{44}N_{16}P + 116\ O_2 + 92\ CO_3^{2-} + 46\ H_2O \longrightarrow 198\ HCO_3^- + 16\ NH_4^+ + HPO_4^{2-}$$

$NH_4^+ + 3/2\ O_2 \longrightarrow NO_2^- + H_2O + 2H^+$

$NH_4^+ + 1/2\ O_2 \longrightarrow NH_2OH + H^+$

$NH_2OH + O_2 \longrightarrow NO_2^- + H_2O + H^+$

$2\ NH_2OH + O_2 \longrightarrow N_2O + 3H_2O$

nitrification, phase I (*nitrosomonas*)

$NO_2^- + 1/2\ O_2 \longrightarrow NO_3^-$

nitrification, phase II ***(nitrosococcus)***

$$C_{106}H_{171}O_{44}N_{16}P + 148\ O_2 + 124\ CO_3^{2-} + 30\ H_2O \longrightarrow 106\ HCO_3^- + 16\ NO_3^- + HPO_4^{2-}$$

stoichiometry of the mineralization of biogenic materials

aerobic mineralization of biogenic materials

nitrification

variable	initial	ΔCorg=-106	final
$\sum CO_2$ (μmol·kg^{-1})	2100	+106	2206
A (μmol·kg^{-1})	2348	-16	2232
pH	8.00	-0.27	7.73
$[CO_2]$ (μmol·kg^{-1})	13.8	+14.1	28.0
$[HCO_3^-]$ (μmol·kg^{-1})	1917	+163	2079
$[CO_3^{2-}]$ (μmol·kg^{-1})	170	-71	99
Ω_{ARG}	2.6		1.5
Ω_{CAL}	4.1		2.4
$pCO_2(g)$ (μatm)	370	+377	747
$[O_2]$ (μmol·kg^{-1})	248	-148	100

stoichiometry and buffering capacity

aerobic mineralization of biogenic materials
nitrification

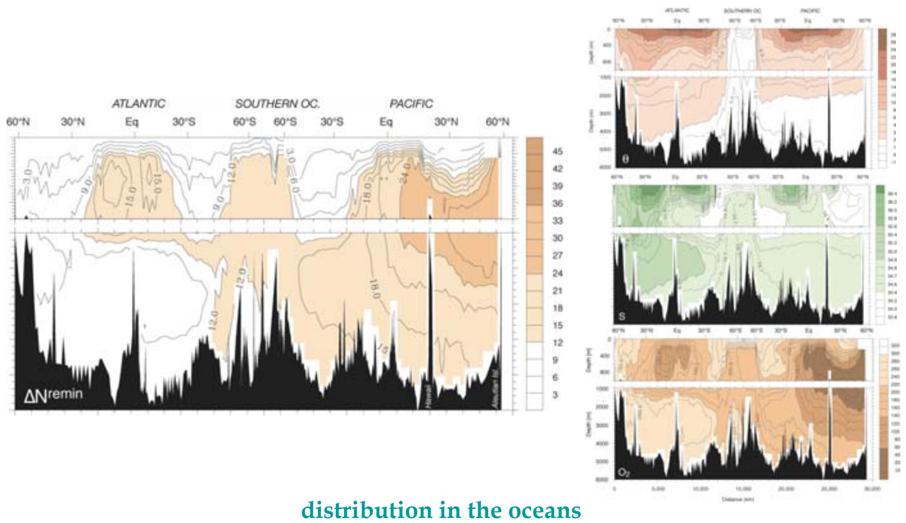

distribution in the oceans

Sarmiento & Gruber, 2006 (http://www.up.ethz.ch/people/ngruber/publications/textbook)

anaerobic mineralization of biogenic materials
denitrification

$C_{106}H_{171}O_{44}N_{16}P + 102{,}4\ NO_3^- \longrightarrow 106\ HCO_3^- + 59{,}2\ N_2\uparrow + HPO_4^{2-} + 29{,}2\ H_2O + 5{,}6\ H^+$

+

$CO_3^{2-} + H^+ \Leftrightarrow HCO_3^-$

NO_3^- is consumed quickly!

$C_{106}H_{171}O_{44}N_{16}P + 102{,}4\ NO_3^- + 5{,}6\ CO_3^{2-} \longrightarrow 111{,}6\ HCO_3^- + 59{,}2\ N_2 + HPO_4^{2-} + 29{,}2\ H_2O$

stoichiometry of the mineralization of biogenic materials

anaerobic mineralization of biogenic materials
denitrification

variable	initial	ΔCorg= -21	final
$\sum CO_2$ (µmol·kg^{-1})	2279	+21	2300
A (µmol·kg^{-1})	2321	+20	2341
pH	7.69	-0.04	7.65
$[CO_2]$ (µmol·kg^{-1})	50.7	+0.4	51.1
$[HCO_3^-]$ (µmol·kg^{-1})	2169	+19	2188
$[CO_3^{2-}]$ (µmol·kg^{-1})	59.3	+0.5	59.8
Ω_{ARG}	0.91		0.92
Ω_{CAL}	1.43		1.44
pCO_2(g) (µatm)	1353	12	1365
$[O_2]$ (µmol·kg^{-1})	0	0	0

stoichiometry and buffering capacity

anaerobic mineralization of biogenic materials
denitrification

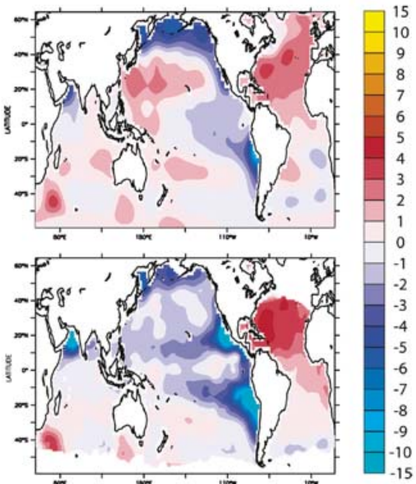

Figure 8. Global distribution of N* (N* = [nitrate] − 16·[phosphate] + 2.9) in the surface ocean (0–100 m, panel a) and along a surface of constant density (1026.6 kg/m³, panel b), based on data from the World Ocean Circulation Experiment.

global distribution in the oceans

anaerobic mineralization of biogenic materials

denitrification

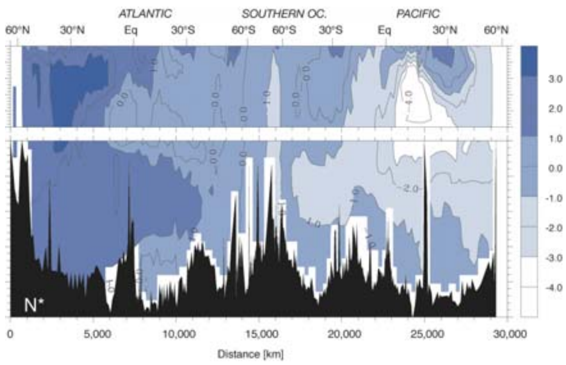

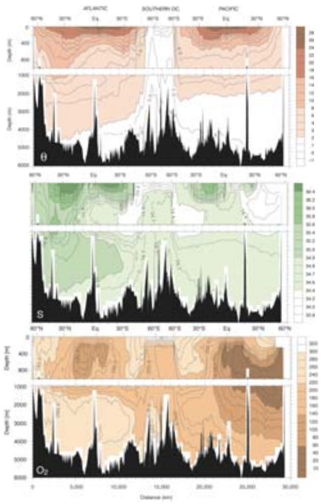

global distribution in the oceans

---

anaerobic mineralization of biogenic materials

anaerobic ammonium oxidation

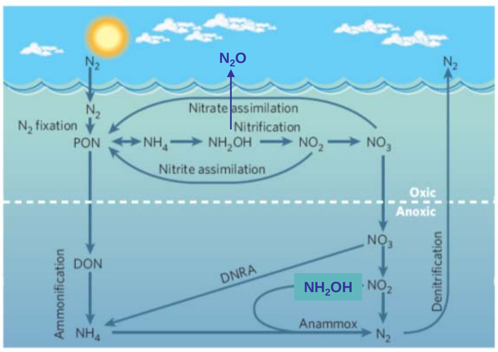

Figure 4 | Marine N cycle, including losses of ammonium and nitrite as N_2 owing to anammox. PON, particulate organic nitrogen, including phytoplankton; DON, dissolved organic nitrogen, DNRA, dissimilatory nitrate reductase to ammonium.

$$NH_4^+ + NO_2^- \rightarrow N_2\uparrow + 2\,H_2O$$

i) $NO_2^- + 2\,NH_4^+ + H_2O \rightarrow 3\,NH_2OH + H^+$ (hidoxilamina)

~~$2\,NH_2OH + O_2 \rightarrow N_2O\uparrow + 3H_2O$~~

ii) $NH_2OH + NH_4^+ \rightarrow N_2H_4 + H_2O + H^+$ (hidrazina)

iii) $3\,N_2H_4 + 4\,H^+ \rightarrow N_2\uparrow + 4\,NH_4^+$

the new route: anammox

Ward et al., Oceanography, 2007

anaerobic mineralization of biogenic materials

sulphate-reduction

$$C_{106}H_{171}O_{44}N_{16}P + 58\ SO_4^{2-} + 46\ H_2O \longrightarrow 106\ HCO_3^- + 16\ NH_4^+ + HPO_4^{2-} + 58\ HS^- + 34\ H^+$$

+

$$CO_3^{2-} + H^+ \Leftrightarrow HCO_3^-$$

$$C_{106}H_{171}O_{44}N_{16}P + 58\ SO_4^{2-} + 34\ CO_3^{2-} + 46\ H_2O \longrightarrow 140\ HCO_3^- + 16\ NH_4^+ + HPO_4^{2-} + 58\ HS^-$$

stoichiometry of the mineralization of biogenic materials

anaerobic mineralization of biogenic materials

sulphate-reduction

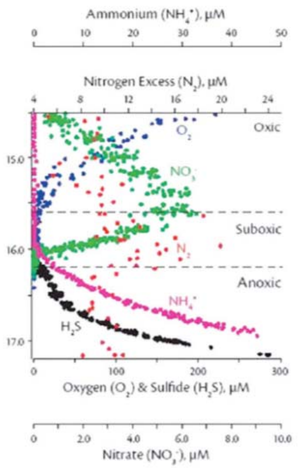

distribution in the oceans

anaerobic mineralization of biogenic materials

fermentation

$$C_{106}H_{171}O_{44}N_{16}P + 104\ H_2O \longrightarrow 58\ CH_4\uparrow + 48\ HCO_3^- + 16\ NH_4^+ + HPO_4^{2-} + 34\ H^+$$

+

$$CO_3^{2-} + H^+ \Leftrightarrow HCO_3^-$$

$$C_{106}H_{171}O_{44}N_{16}P + 34\ CO_3^{2-} + 104\ H_2O \longrightarrow 58\ CH_4\uparrow + 82\ HCO_3^- + 16\ NH_4^+ + HPO_4^{2-}$$

stoichiometry of the mineralization of biogenic materials

anaerobic mineralization of biogenic materials

fermentation

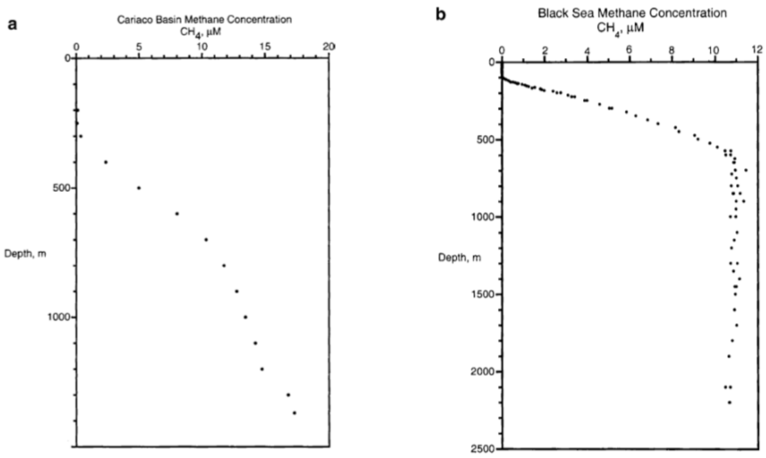

distribution in the oceans

Reeburgh, Chem. Rev., 2007

anaerobic mineralization of biogenic materials

procceses in the sediments

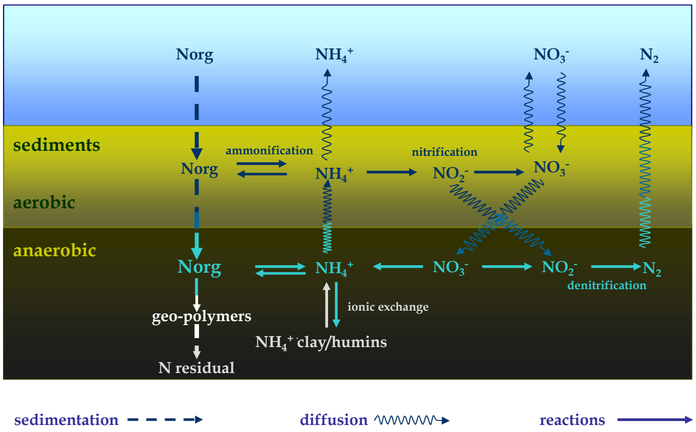

Klump & Martens, 1983

anaerobic mineralization of biogenic materials

procceses in the sediments

Eh (Volts)

aerobia

Amonificación

$C_{106}H_{171}O_{44}N_{16}P + 116\ O_2\uparrow + 46\ H_2O \longrightarrow 106\ HCO_3^- + 16\ NH_4^+ + HPO_4^{2-} + 92\ H^+$

Nitrificación

$C_{106}H_{171}O_{44}N_{16}P + 148\ O_2\uparrow + 30\ H_2O \longrightarrow 106\ HCO_3^- + 16\ NO_3^- + HPO_4^{2-} + 124\ H^+$ — +0,20 /+0,80

anaerobia

Semi-par reductor (donante de e-)

$C_{106}H_{171}O_{44}N_{16}P + 278\ H_2O \longrightarrow 106\ HCO_3^- + 16\ NH_4^+ + HPO_4^{2-} + 556\ H^+ + 464\ e^-$

Semi-par oxidante (aceptor de e-)

		Eh (Volts)
desnitrificación	$2\ NO_3^- + 6\ H_20 + 10\ e^- \longrightarrow N_2\uparrow + 12\ OH^-$	+0,05 /+0,75
Mn(IV)	$MnO_2 + 4\ H^+ + 2\ e^- \longrightarrow Mn^{2+} + 2\ H_2O$ *(birnesita, nsutita ó pirolusita)*	+0,10 /+0,60
$NO_3^- \rightarrow NH_4^+$	$NO_3^- + 7\ H_2O + 8\ e^- \longrightarrow NH_4^+ + 10\ OH^-$	-0,20 /+0,40
Fe(III)	$Fe_2O_3 + 6\ H^+ + 2\ e^- \longrightarrow 2\ Fe^{+2} + 3\ H_2O$ *(hematita)* $FeOOH + 3\ H^+ + 1e^- \longrightarrow Fe^{2+} + 2\ H_2O$ *(geotita)*	-0,50 /+0,05
sulfato reducción	$SO_4^{2-} + 5\ H_2O + 8\ e^- \longrightarrow HS^- + 9\ OH^-$	-0,65 /-0,20
fermentación	$CO_2\uparrow + 8\ H^+ + 8\ e^- \longrightarrow CH_4\uparrow + 2\ H_2O$	

profundidad ↓

anaerobic mineralization of biogenic materials

procceses in the sediments

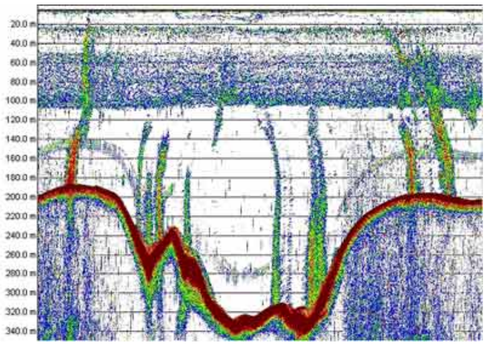

methane in coastal sediments

Kaudla & Sandler, Energy & Fuel, 2005

mineralization of inorganic biogenic materials

mineralization of biogenic silica

$$SiO_2 \cdot nH_2O_{(s)} \longrightarrow H_4SiO_4 + (n\text{-}2)\ H_2O$$

stoichiometry of the mineralization of biogenic materials

mineralization of inorganic biogenic materials

mineralization of biogenic silica

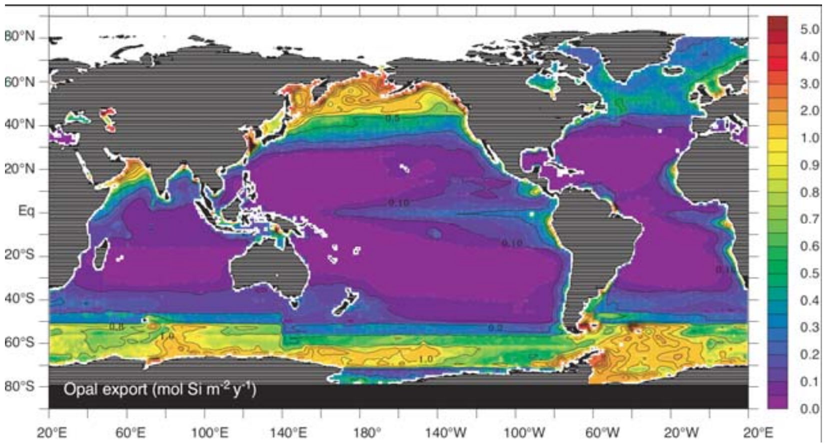

global distribution of BSi disolution in the oceans

mineralization of inorganic biogenic materials

mineralization of calcareous structures

$$CaCO_3\,(s) \longrightarrow CO_3^{2-} + Ca^{2+}$$

stoichiometry of the mineralization of biogenic materials

mineralization of inorganic biogenic materials

mineralization of calcareous structures

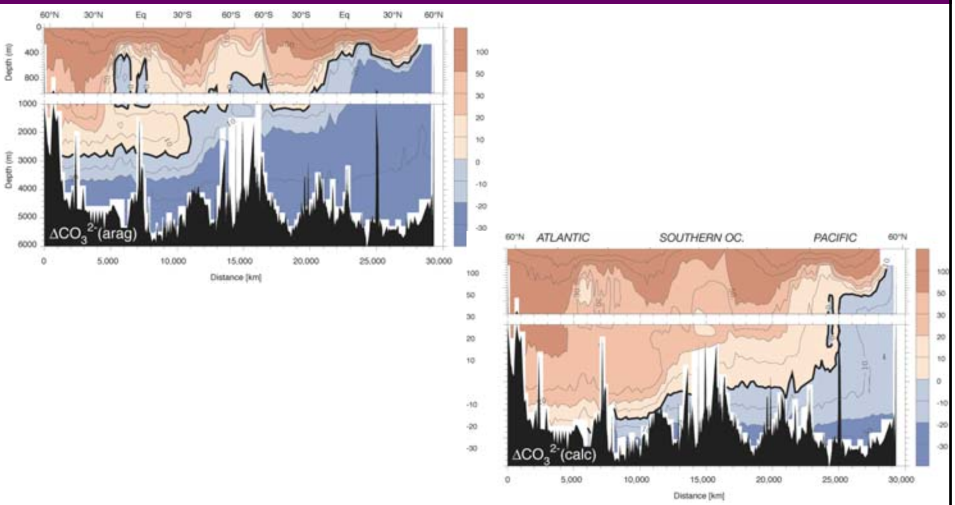

global distribution of $CaCO_3$ dissolution in the oceans

Sarmiento & Gruber, 2006 (http://www.up.ethz.ch/people/ngruber/publications/textbook)

Impact of global change on ocean biogeochemical cycles (N, P, C and trace elements)
Palma de Mallorca, 4 – 8 Nov 2013

IV. Ocean biogeochemical cycles

X. Antón Álvarez Salgado
CSIC, Instituto de Investigacións Mariñas
C/ Eduardo Cabello 6, 36208 - Vigo
http://www.iim.csic.es

outline of this presentation

ocean biogeochemical cycles

- **the biological pump: before (1980's) and after (1990's)**
- **cycling of biogenic organic matter: nitrogen and phosphorus in the oceans**
- **cycling of biogenic inorganic matter: silicon and calcium carbonate**

the biological pump in the oceans

the biological pump in the 1980's

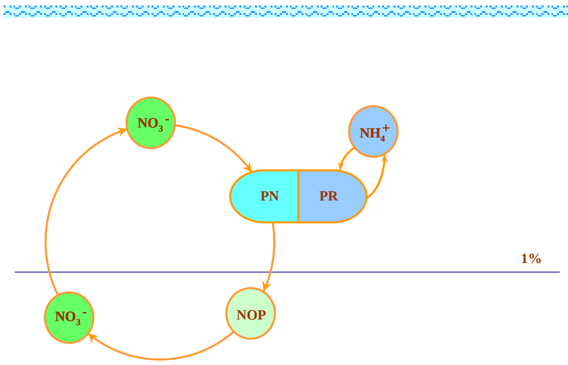

Eppley & Petersen (1979) model

the biological pump in the oceans

the biological pump in the 1980's

$^{15}NO_3^-$, $^{15}NH_4^+$

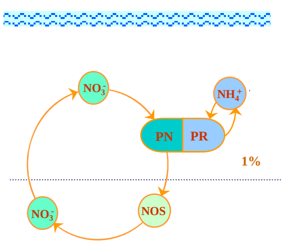

sediment traps

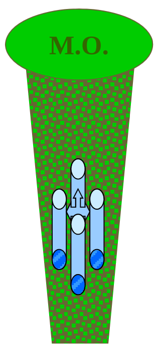

geochemical budgets

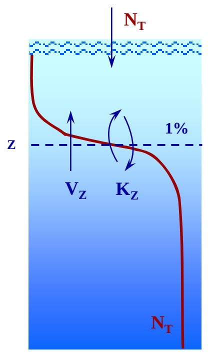

new or exportable production estimates

the biological pump in the oceans
the biological pump in the 1980's

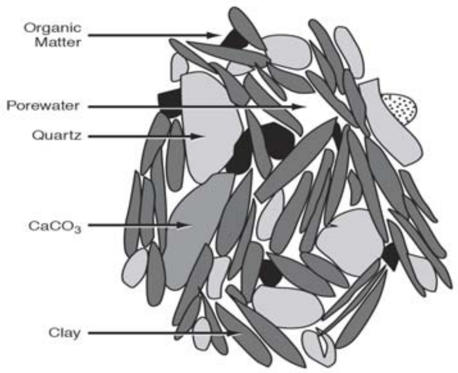

new or exportable production estimates

Sarmiento & Gruber, 2006 (http://www.up.ethz.ch/people/ngruber/publications/textbook)

the biological pump in the oceans
the biological pump in the 1980's

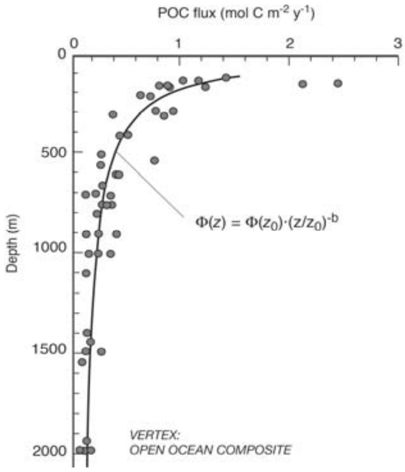

sediment traps

Sarmiento & Gruber, 2006 (http://www.up.ethz.ch/people/ngruber/publications/textbook)

the biological pump in the oceans

the biological pump in the 1980's

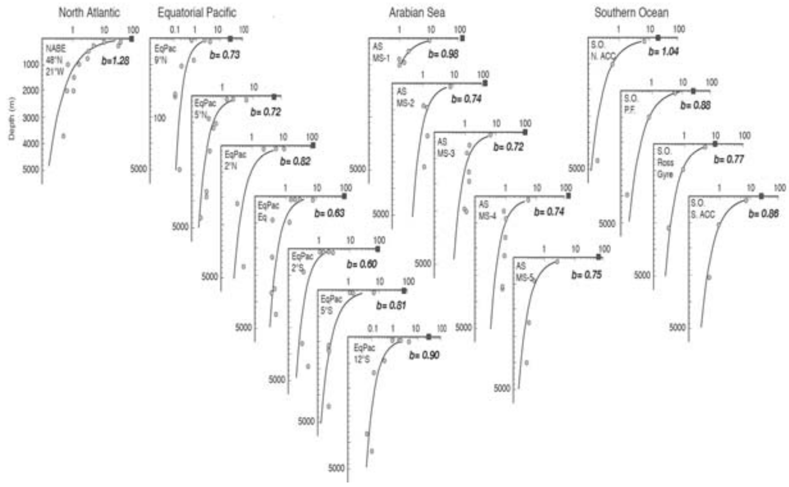

sediment traps

Sarmiento & Gruber, 2006 (http://www.up.ethz.ch/people/ngruber/publications/textbook)

the biological pump in the oceans

the biological pump in the 1980's

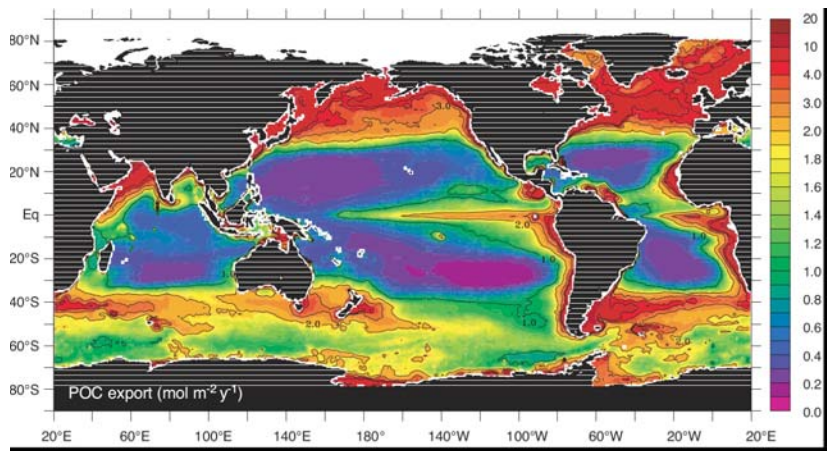

sediment traps: fluxes at the epi-mesopelagic interface (150 m)

Sarmiento & Gruber, 2006 (http://www.up.ethz.ch/people/ngruber/publications/textbook)

the biological pump in the oceans

the biological pump in the 1980's

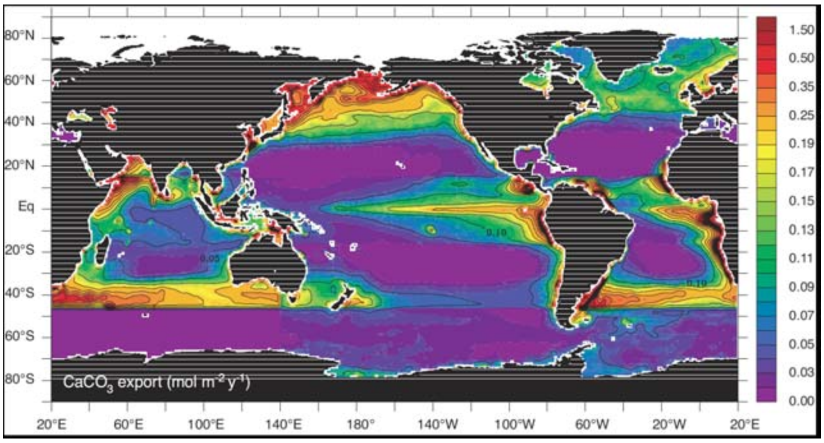

sediment traps: fluxes at the epi-mesopelagic interface (150 m)

Sarmiento & Gruber, 2006 (http://www.up.ethz.ch/people/ngruber/publications/textbook)

the biological pump in the oceans

the biological pump in the 1980's

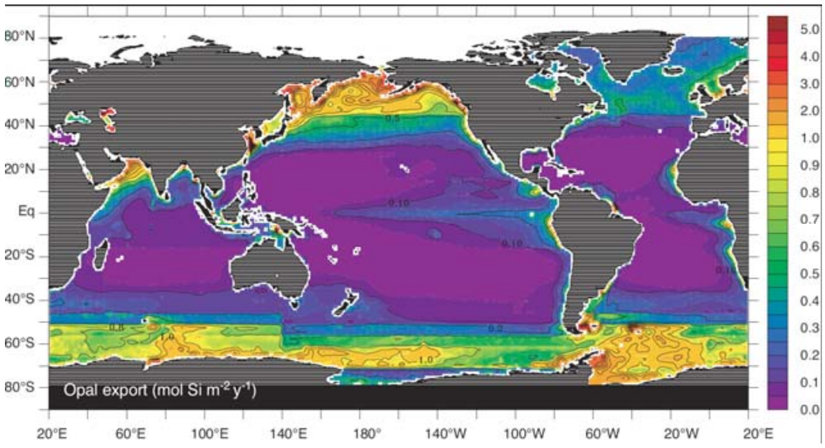

sediment traps: fluxes at the epi-mesopelagic interface (150 m)

Sarmiento & Gruber, 2006 (http://www.up.ethz.ch/people/ngruber/publications/textbook)

the biological pump in the oceans

the biological pump in the 1980's

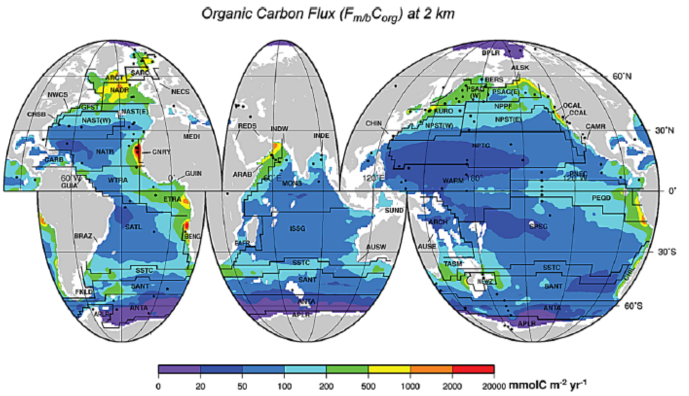

Fig. 9. Global parameterization of $F_{2\,km}C_{org}$ in mmolC m^{-2} yr^{-1} based on individual TS-trap data sets from four model domains—the Trade Wind Domain (as in Longhurst et al., 1995), the Arabian Sea Region, the Antarctic Zone, and data from default stations—projected on the geography of biogeochemical provinces and stations that were used for analyzing the data presented in this paper.

sediment traps: fluxes at the meso-batipelagic interface (2 Km)

Honjo et al.., Prog. Oceanogr., 2008

the biological pump in the oceans

the biological pump in the 1980's

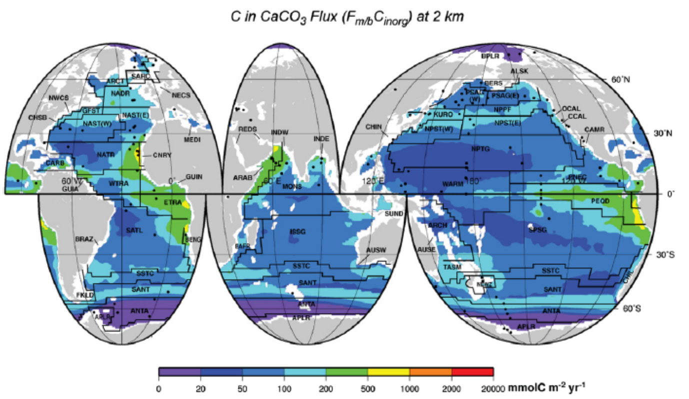

Fig. 10. Global parameterization of $F_{m/b}C_{inorg}$ in mmolC m^{-2} yr^{-1} based on individual TS-trap data sets from four model domains as in Fig. 9.

sediment traps: fluxes at the meso-batipelagic interface (2 Km)

Honjo et al.., Prog. Oceanogr., 2008

the biological pump in the oceans
the biological pump in the 1980's

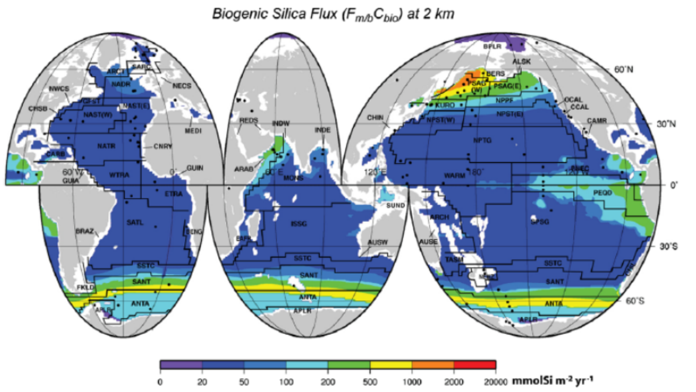

Fig. 11. Global parameterization of $F_{m/b}Si_{bio}$ in mmolSi m^{-2} yr^{-1} based on individual TS-trap data sets from four model domains as in Fig. 9.

sediment traps: fluxes at the meso-batipelagic interface (2 Km)

Honjo et al.., Prog. Oceanogr., 2008

the biological pump in the oceans
the biological pump in the 1980's

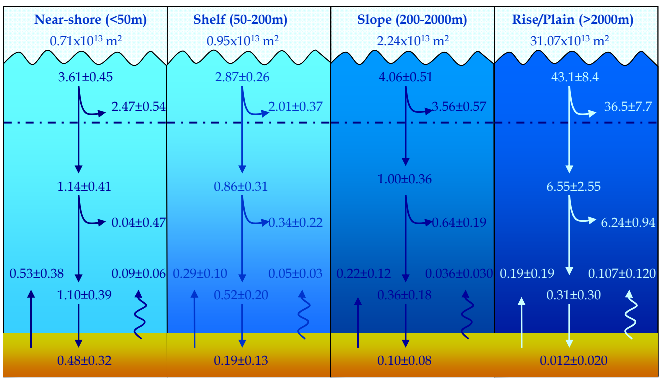

sediment traps: summary of organic carbon fluxes (Pg C/a)

Dunne et al.., Global Biogeochem. Cy., 2007

the biological pump in the oceans

the biological pump in the 1980's

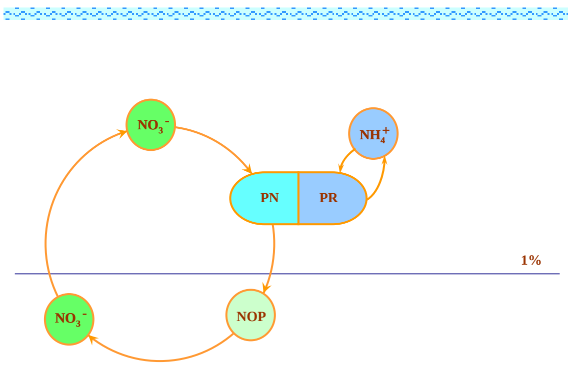

atmospheric inputs

the biological pump in the oceans

the biological pump in the 1980's

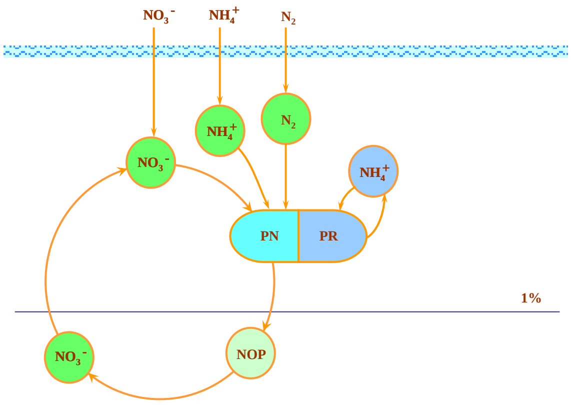

atmospheric inputs

the biological pump in the oceans
the biological pump in the 1990's

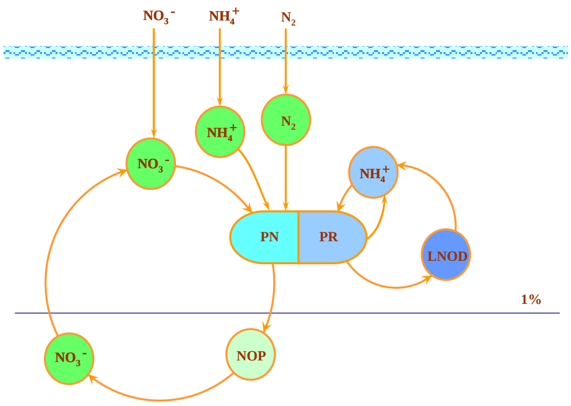

l-DOM: recycled in hours-days

the biological pump in the oceans
the biological pump in the 1990's

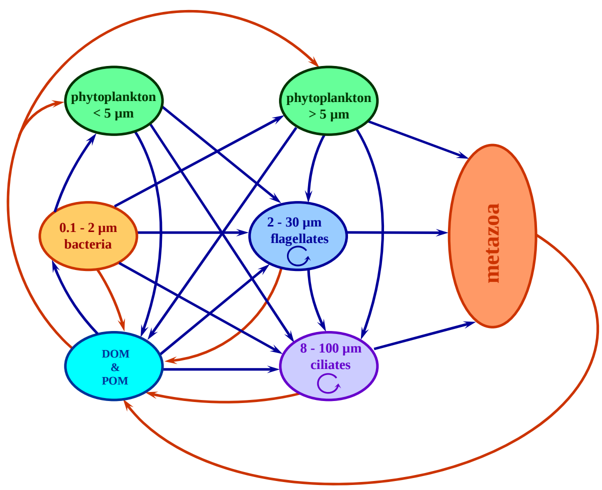

l-DOM: recycled in hours-days

Sherr & Sherr, Limnol. Oceanogr., 1989

the biological pump in the oceans

the biological pump in the 1990's

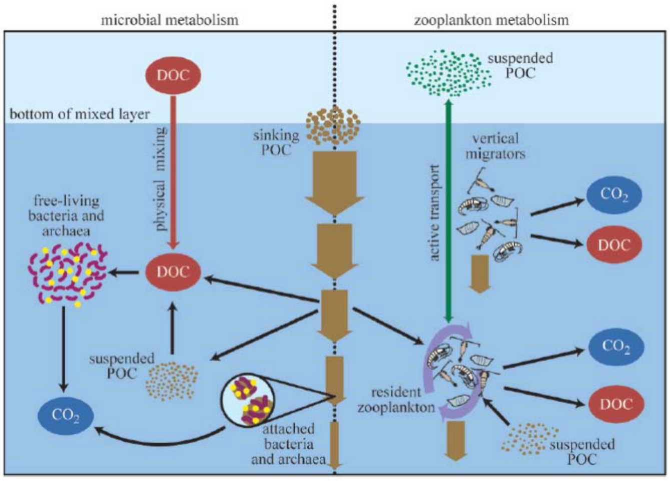

l-DOM: recycled in hours-days

Steinberg et al., Limnol. Oceanogr., 2008

the biological pump in the oceans

the biological pump in the 1990's

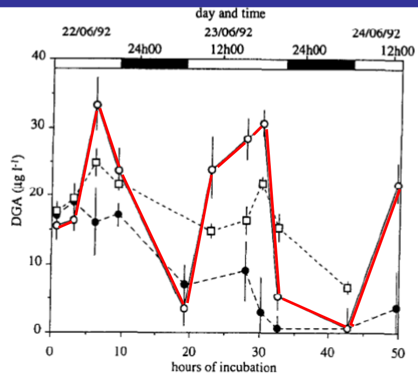

Fig. 1. Evolution of dissolved glycolate concentrations in closed bottles of unenriched natural sea water. Water was taken at 139 m depth at the oligotrophic site, eastern Atlantic Ocean, and filtered on 200 µm mesh to remove large particles and grazers. Open circles and bold lines are for the natural surface light incubations; open squares and dashed lines are for 1% light irradiance bottles; and closed circles and dashed lines are for the dark incubation. Beginning of the experiment was at 10h00, June 23, 1992, and night periods are marked by black bands. Errors bars = SE (3σ).

l-DOM: recycled in hours-days

Leboulanger et al., Deep-Sea Res., 1995

the biological pump in the oceans

the biological pump in the 1990's

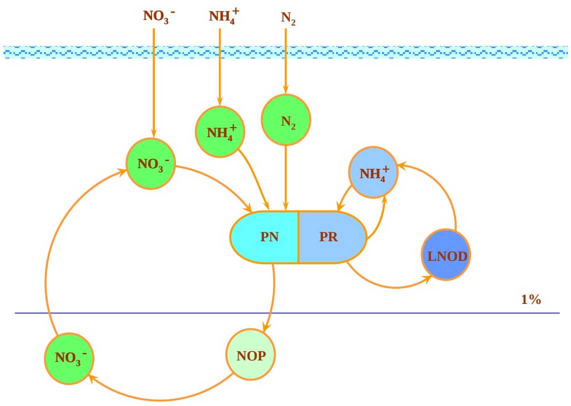

s-DOM: recycling in weeks-months

the biological pump in the oceans

the biological pump in the 1990's

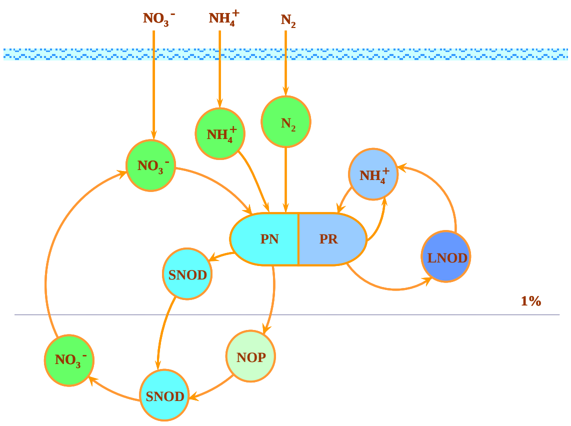

s-DOM: recycling in weeks-months

the biological pump in the oceans

the biological pump in the 1990's

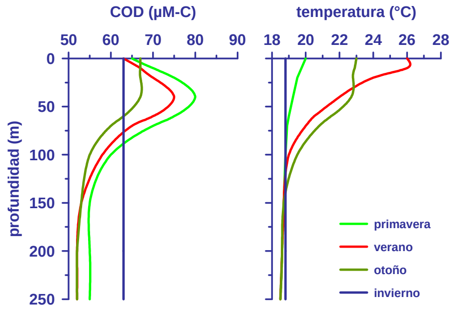

s-DOM: recycling in weeks-months

Carlson et al., Nature, 1994

the biological pump in the oceans

the biological pump in the 1990's

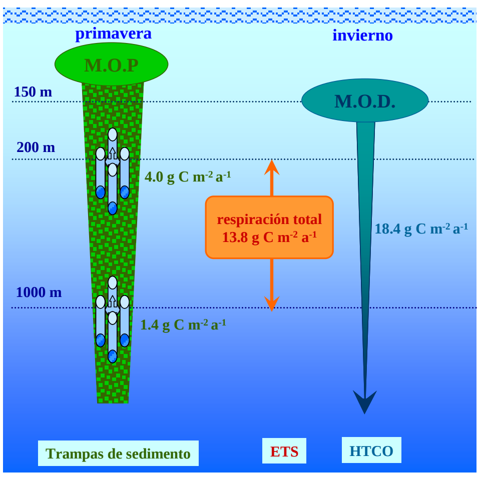

s-DOM: recycling in weeks-months

Lefevre et al., J. Mar. Sys., 1996

the biological pump in the oceans

the biological pump in the 1990's

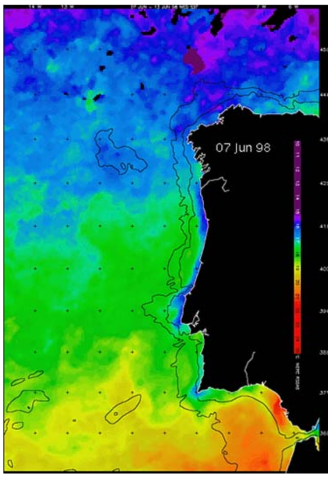

s-DOM: recycling in weeks-months

Álvarez-Salgado et al., Limnol. Oceanogr., 2007

the biological pump in the oceans

the biological pump in the 1990's

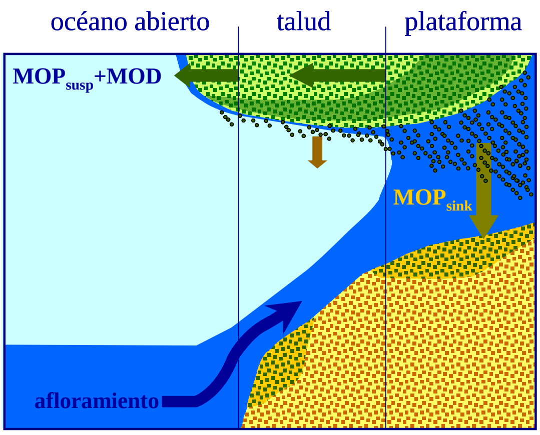

s-DOM: recycling in weeks-months

Álvarez-Salgado et al., Limnol. Oceanogr., 2007

the biological pump in the oceans

the biological pump in the 1990’s

Table 1. Compilation from published dissolved and suspended particulate organic carbon (DOC, POC) and total inorganic nitrogen (N_T) concentrations in upwelled (up; average of 100–200 m depth range) and surface outwelled (out; upper 50 m off Iberia and upper 100 m off NW Africa) waters of the study filaments at the shelf break; DOC and POC excesses (ΔDOC, ΔPOC) and inorganic carbon deficit (ΔC_T) in shelf-break surface waters; percentage of the exported organic material in the dissolved form (ΔDOC/[ΔDOC + ΔPOC]) and percentage of the new production that is exported off shelf ($-[\Delta DOC + \Delta POC]/\Delta C_T$); volume transport (VT) of shelf surface water and organic carbon flux (C flux) exported by the filaments (annual basis); area (A) of the shelf that is exported by each upwelling filament; primary production in that area (PP), and the percentage of PP exported by the filaments (−[ΔDOC + ΔPOC]/PP); filament : Ekman transport ratio (dimensionless).

		NW Iberia	NW Africa	
		42°–43°N	30°–31°N	26°–28°N
Period		Apr–Sep 1995	Sep–Oct 1997	Aug 1999
DOC (μmol L^{-1})	Up	63.0*	51.0†	60.0‡
	Out	78.6*	75.6†	90.0‡
POC (μmol L^{-1})	Up	1.4*	0.8†	1.7‡
	Out	10.1*	2.1†	6.0‡
N_T (μmol L^{-1})	Up	9.5*	10.0†	8.0‡
	Out	0.1*	0.1†	0.1‡
ΔDOC (μmol L^{-1})		15.6	24.6	30
ΔPOC (μmol L^{-1})		8.7	1.3	4.3
ΔC_T (μmol L^{-1})		−70	−74	−59
(ΔDOC)/(ΔDOC+ΔPOC)		64%	95%	87%
$-(\Delta DOC+\Delta POC)/\Delta C_T$		35%	35%	58%
VT (m^3 yr^{-1})		1.4×10^{12}§	9.9×10^{12}†	7.5×10^{12}‡
A (km^2)		3,400	6,660	13,400
C flux	(kg C yr^{-1})	4.1×10^{8}	3.1×10^{9}	3.1×10^{9}
	(g C m^{-2} yr^{-1})	120	460	230
PP (g C m^{-2} y^{-1})		630‖	750¶	750¶
(ΔDOC+ΔPOC)/PP		20%	60%	30%
Filament : Ekman transport ratio		2.5	4.4	2.4

* Álvarez-Salgado et al. (1999).
† García-Muñoz et al. (2005).
‡ García-Muñoz et al. (2004).
§ Álvarez-Salgado et al. (2001).
‖ Arístegui et al. (2006).
¶ Longhurst et al. (1995).

s-DOM: recycling in weeks-months

Álvarez-Salgado et al., Limnol. Oceanogr., 2007

the biological pump in the oceans

the biological pump in the 1990’s

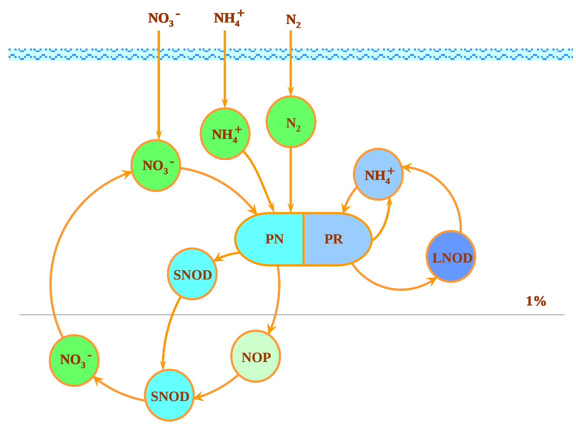

r-DOM: recycling in years-millennia

the biological pump in the oceans

the biological pump in the 1990's

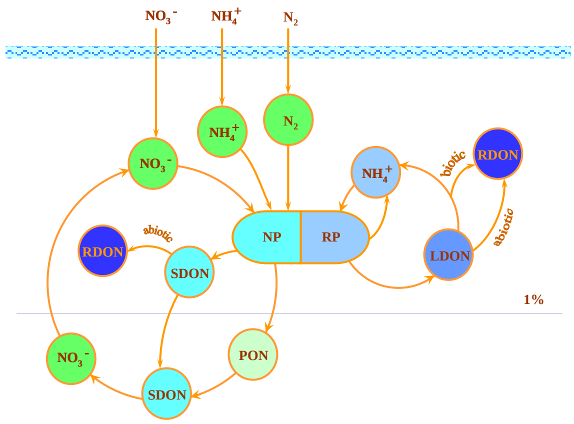

r-DOM: recycling in years-millennia

the biological pump in the oceans

the biological pump in the 1990's

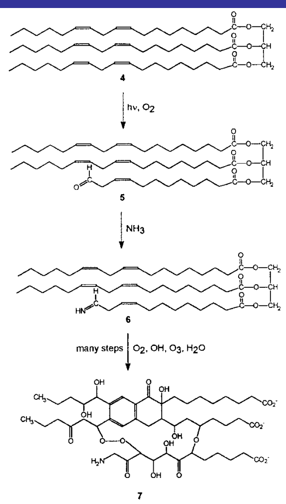

r-DOM: recycling in years-millennia: abiotic processes

Kieber et al.L Limnol. Oceanogr. 1997

the biological pump in the oceans
the biological pump in the 1990's

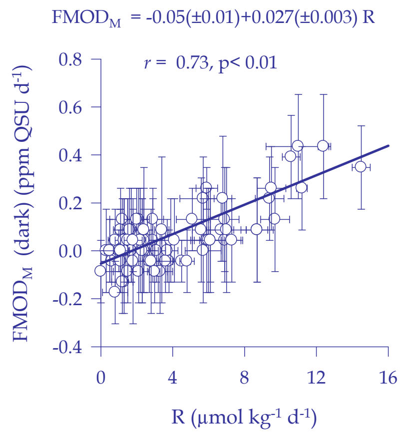

r-DOM: recycling in years-millennia: biotic processes

Nieto-Cid et al., Limnol. Oceanogr., 2006

the biological pump in the oceans
the biological pump in the 1990's

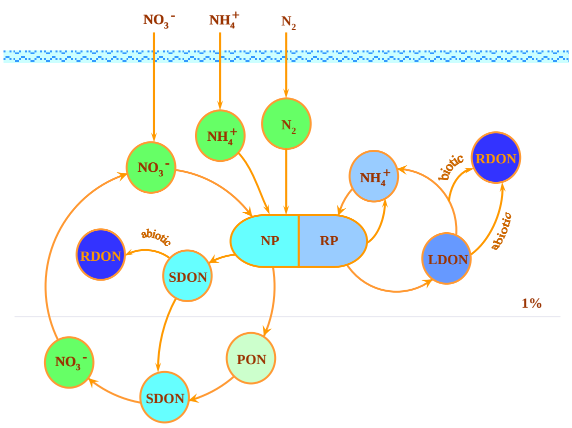

r-DOM: recycling in years-millennia

the biological pump in the oceans

the biological pump in the 1990's

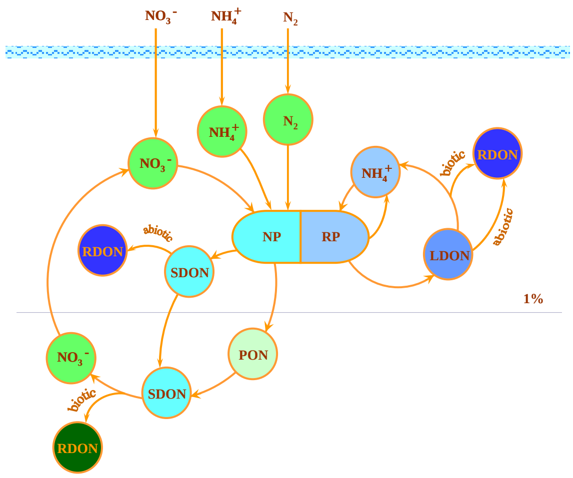

r-DOM: recycling in years-millennia

the biological pump in the oceans

the biological pump in the 1990's

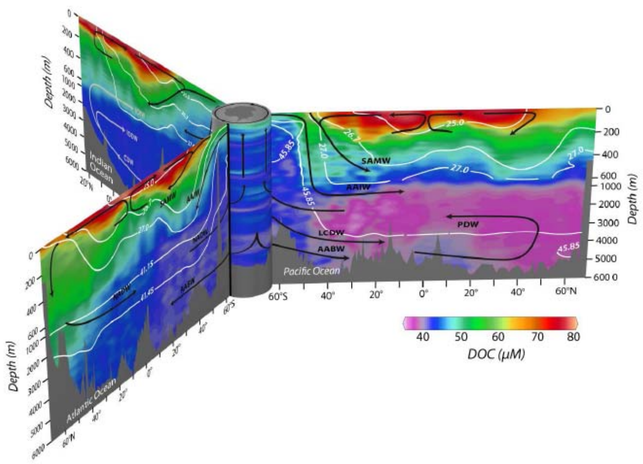

r-DOM: recycling in years-millennia

Hansell et al., Oceanography, 2009

the biological pump in the oceans

the biological pump in the 1990's

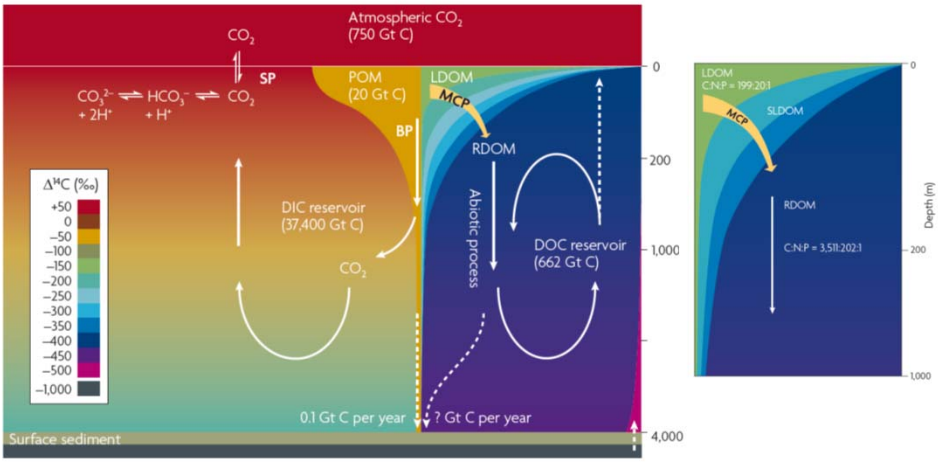

r-DOM: recycling in years-millennia

the biological pump in the oceans

the biological pump in the 1990's

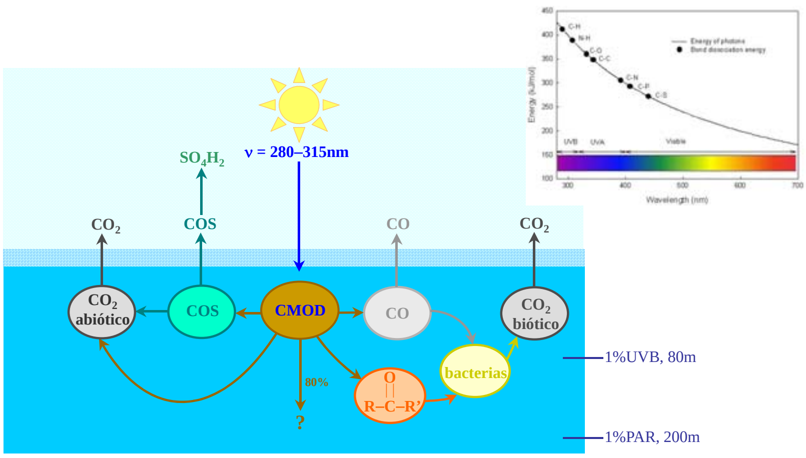

r-DOM: photochemical decomposition in surface waters

Yamashita and Tanoue, Nature, 2008

the biological pump in the oceans
the biological pump in the 1990's

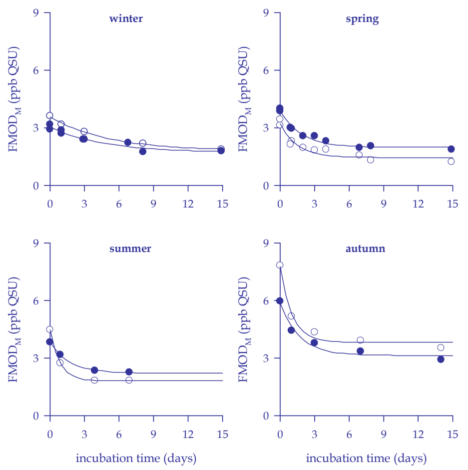

r-DOM: photochemical decomposition in surface waters

Nieto-Cid et al., Limnol. Oceanogr., 2005

the biological pump in the oceans
the biological pump in the 1990's

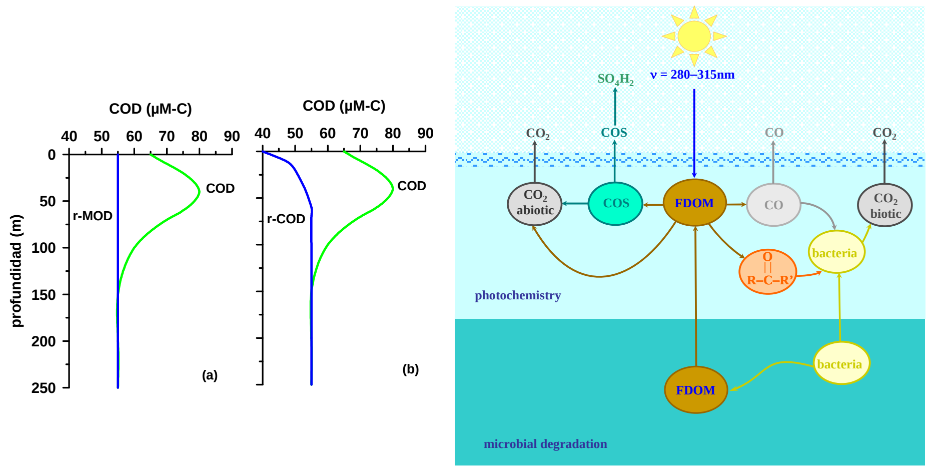

r-DOM: photochemical decomposition in surface waters

Nieto-Cid et al., Limnol. Oceanogr., 2006

the biological pump in the oceans

the biological pump in the 1990’s

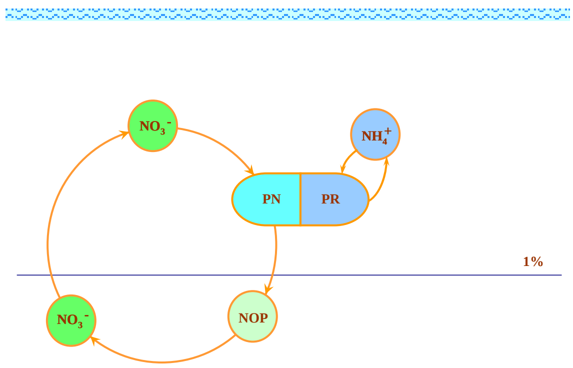

DOM: summarizing

the biological pump in the oceans

the biological pump in the 1990’s

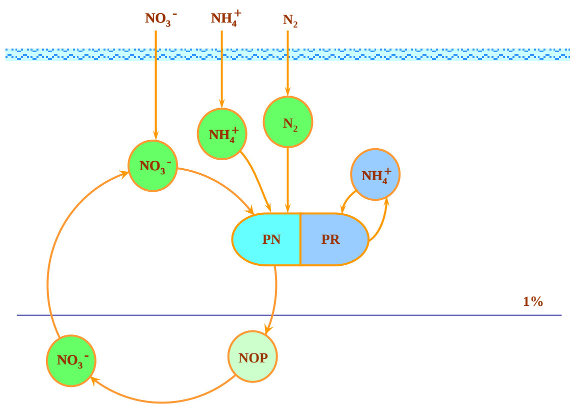

DOM: summarizing

the biological pump in the oceans

the biological pump in the 1990's

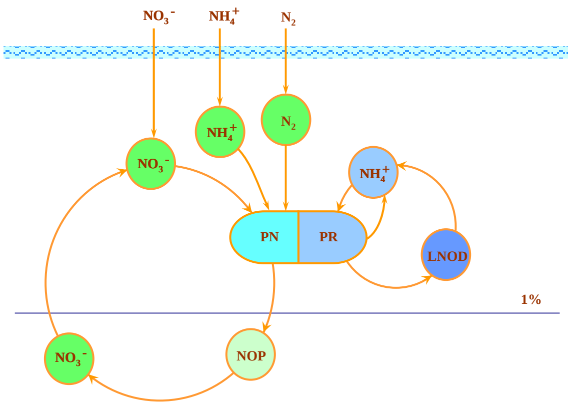

DOM: summarizing

the biological pump in the oceans

the biological pump in the 1990's

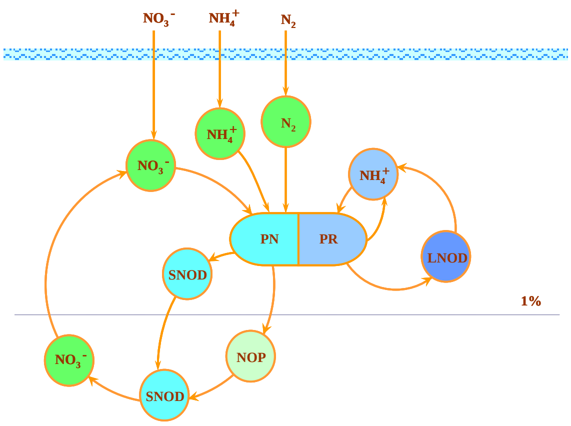

DOM: summarizing

the biological pump in the oceans

the biological pump in the 1990's

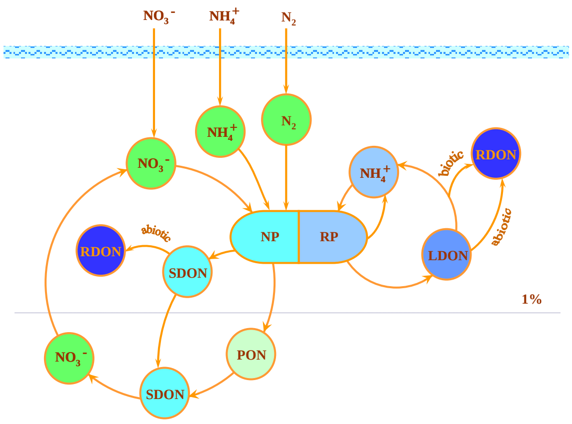

DOM: summarizing

the biological pump in the oceans

the biological pump in the 1990's

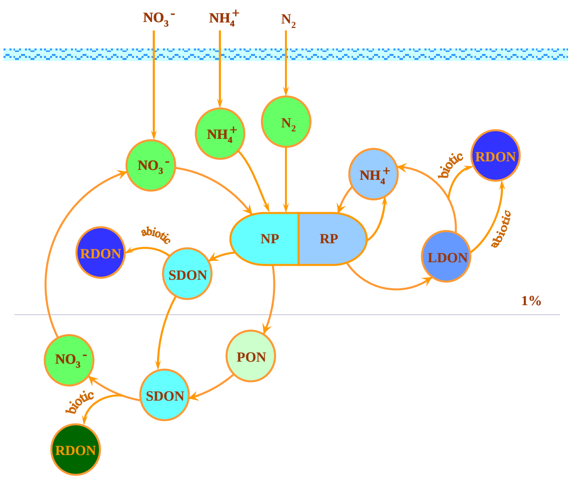

DOM: summarizing

organic matter cycling in the oceans

nitrogen

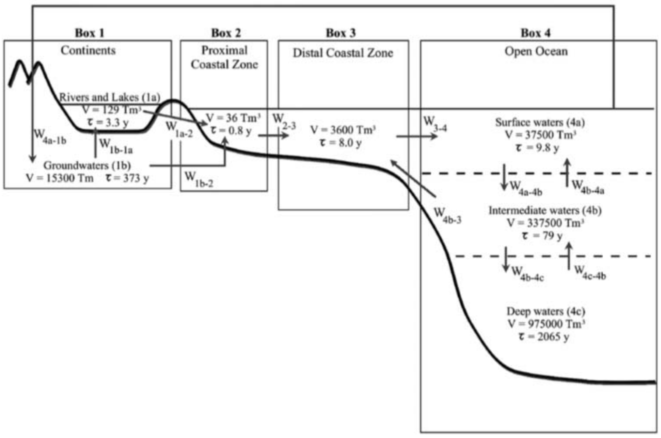

Figure 1. Global Water Cycle with water masses in Tm^3 and water fluxes (W) in Tm^3 yr^{-1}. V, volume; τ, residence time.

open versus coastal ocean

Laurelle et al, Global Biogeochem. Cy., 2009

organic matter cycling in the oceans

nitrogen

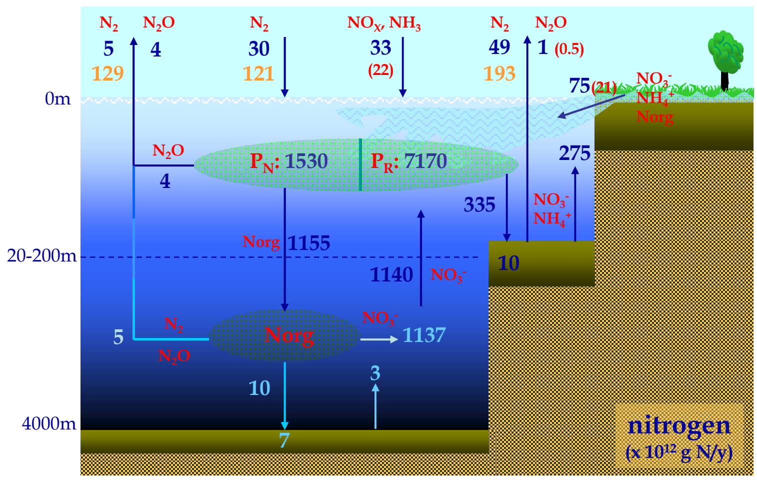

Galloway et al., Biogeochemistry, 2004

Wollast, 1993

organic matter cycling in the oceans
nitrogen

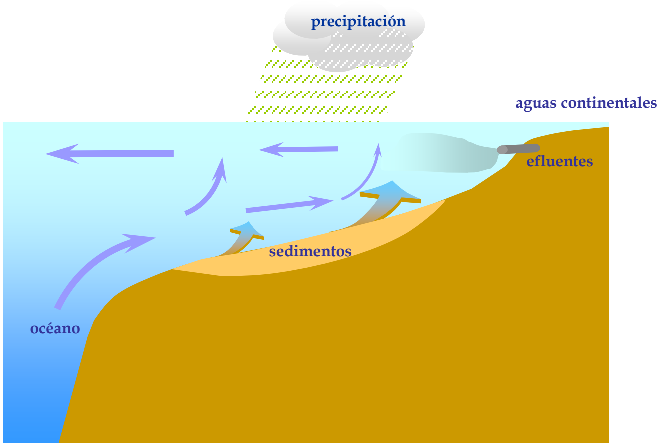

nitrogen cycle in the coastal zone

organic matter cycling in the oceans
nitrogen

- ► represent <10% of the area and <1% of the volume of the oceans
- ► support between 25% and 50% of the global new production
- ► receive 80% of the sedimentation of the oceans
- ► about 90% of the fish resoruces are extracted from the coastal zone

nitrogen cycle in the coastal zone

Gattuso et al., 1998

organic matter cycling in the oceans

nitrogen

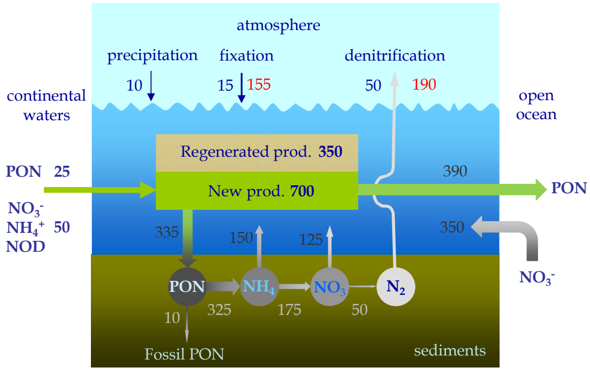

nitrogen cycle in the coastal zone (in 10^{12} gN/y)

Galloway et al., Biogechemistry, 2004

Wollast, 1993

organic matter cycling in the oceans

phosphorus

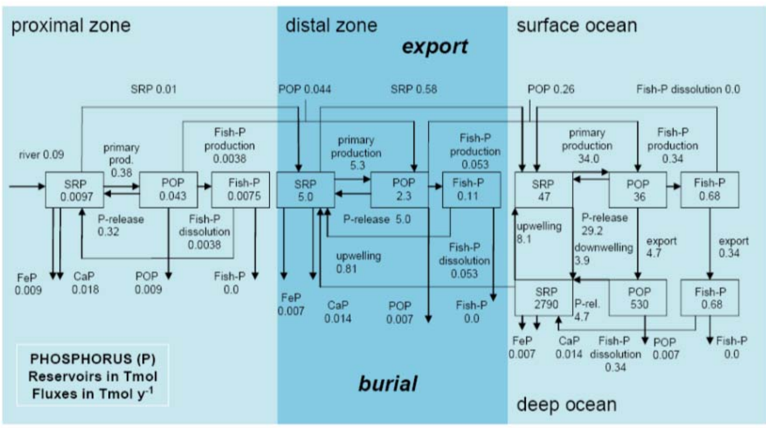

Fig. 2. Modern steady-state oceanic phosphorus (P) cycle. Reservoirs in Tmol; Fluxes in Tmol y^{-1}.

coastal and open ocean phosphorus cycle

Slomp & Van Cappellen, Biogeosciences., 2007

organic matter cycling in the oceans

silicon

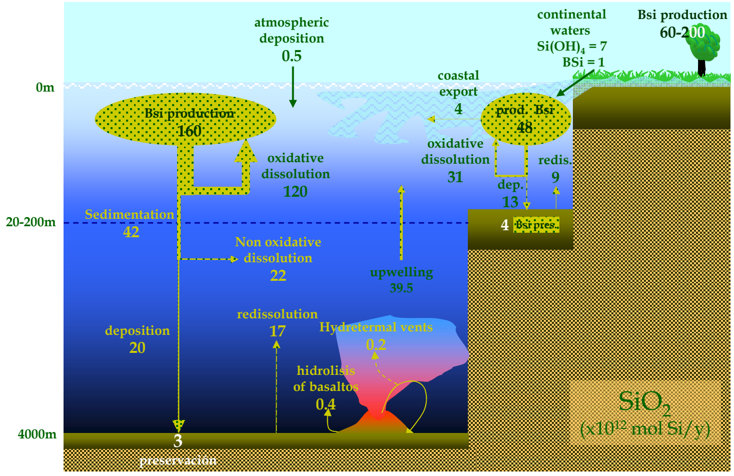

silicon cycle in the open ocean and the coastal zone

Laruelle et al., Global. Biogeochem. Cy, 2009 | Nelson et al., Global. Biogeochem. Cy, 1995

organic matter cycling in the oceans

calcium carbonate

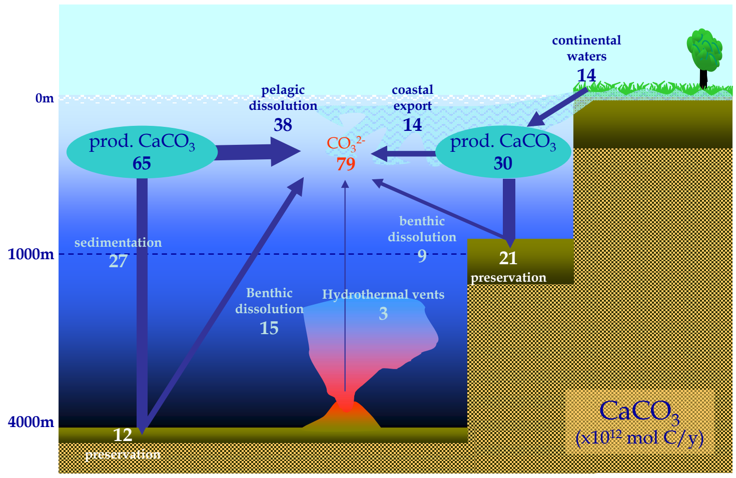

$CaCO_3$ cycle in the ocean and the coastal zone

Wollast, 1994 | Milliman et al., Deep. Sea Res., 1999

Impact of global change on ocean biogeochemical cycles (N, P, C and trace elements)
Palma de Mallorca, 4– 8 Nov 2013

V. Impact of global change on ocean biogeochemical cycles

X. Antón Álvarez Salgado
CSIC, Instituto de Investigacións Mariñas
C/ Eduardo Cabello 6, 36208 - Vigo
http://www.iim.csic.es

outline of this presentation

impact of global change on the ocean biogeochemical cycle of …

- **nitrogen**
- **phosphorus**
- **silicon**

global change and nitrogen in the oceans

mankind: the king of N_2 fixation in the bisophere

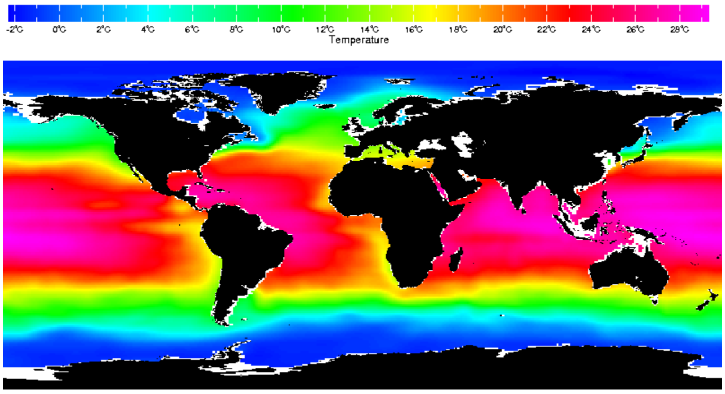

global distribution of surface temperature

http://ingrid.ldgo.columbia.edu/SOURCES/LEVITUS94/

global change and nitrogen in the oceans

mankind: the king of N_2 fixation in the bisophere

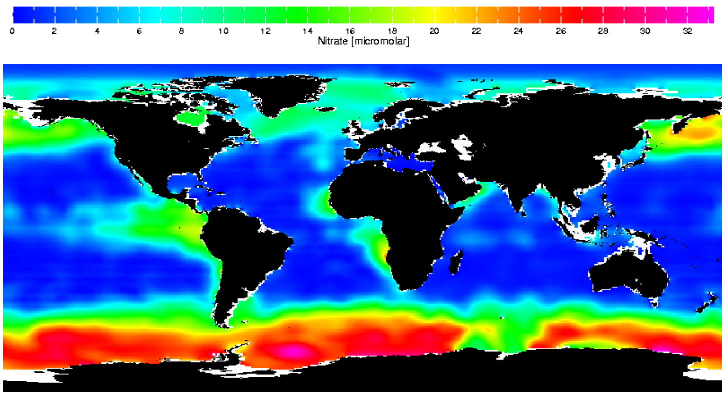

global distribution of nitrate

http://ingrid.ldgo.columbia.edu/SOURCES/LEVITUS94/

global change and nitrogen in the oceans

mankind: the king of N_2 fixation in the bisophere

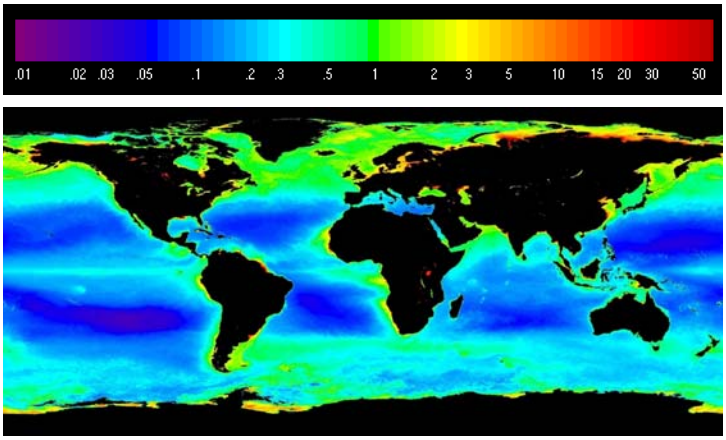

global distribution of chlorophyll

global change and nitrogen in the oceans

mankind: the king of N_2 fixation in the bisophere

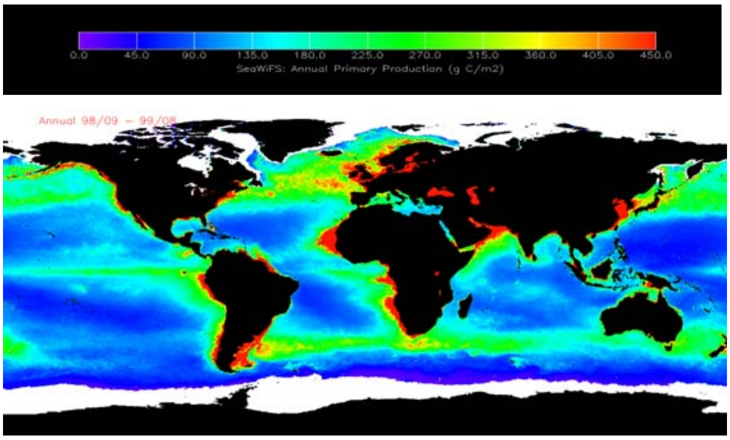

global distribution of primary production

global change and nitrogen in the oceans

mankind: the king of N_2 fixation in the bisophere

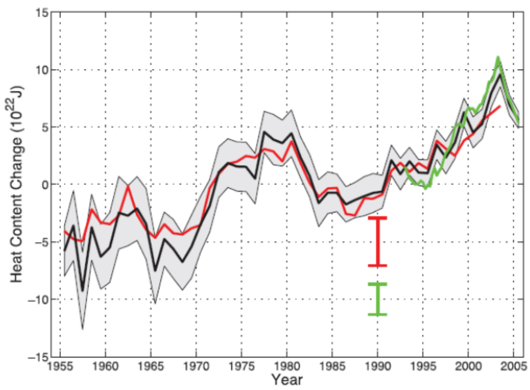

Figure 5.1. *Time series of global annual ocean heat content (10^{22} J) for the 0 to 700 m layer. The black curve is updated from Levitus et al. (2005a), with the shading representing the 90% confidence interval. The red and green curves are updates of the analyses by Ishii et al. (2006) and Willis et al. (2004, over 0 to 750 m) respectively, with the error bars denoting the 90% confidence interval. The black and red curves denote the deviation from the 1961 to 1990 average and the shorter green curve denotes the deviation from the average of the black curve for the period 1993 to 2003.*

heat content of the oceans (0-700m) 1955-2005

http://www.ipcc-wg2.org

global change and nitrogen in the oceans

mankind: the king of N_2 fixation in the bisophere

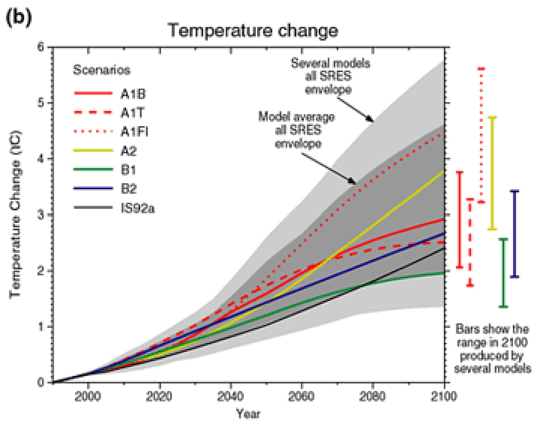

air temperature increase over the next decade

http://www.ipcc-wg2.org

global change and nitrogen in the oceans

mankind: the king of N_2 fixation in the bisophere

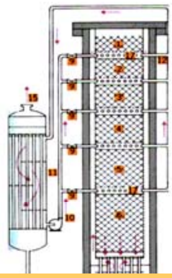

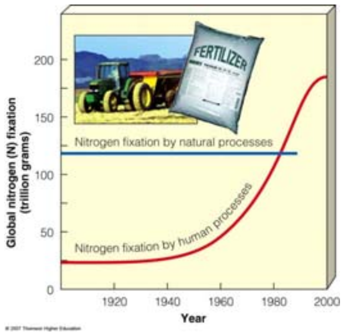

$3\,CH_4 + 6\,H_2O \longrightarrow 3\,CO_2 + 12\,H_2$

$4\,N_2 + 12\,H_2 \longrightarrow 8\,NH_3$

$3\,CH_4 + 4N_2 + 6\,H_2O \longrightarrow 3\,CO_2 + 8\,NH_3$

global change and nitrogen in the oceans

mankind: the king of N_2 fixation in the bisophere

% cultivo cerelaes

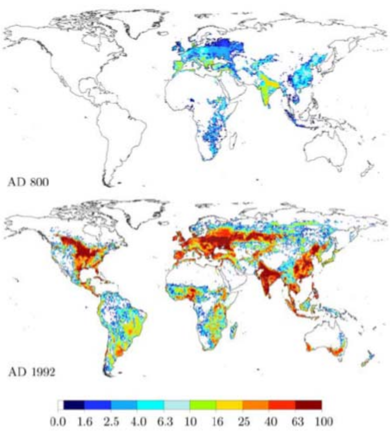

% pastizales

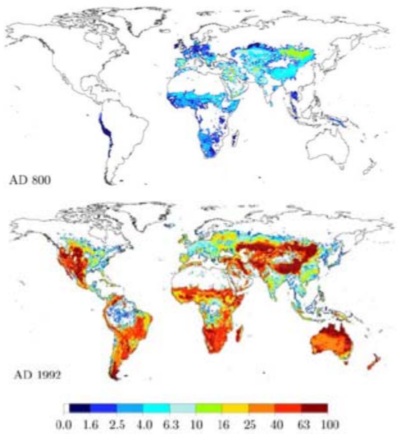

Pongratz et al., Global Biogeochem Cy, 2009

global change and nitrogen in the oceans

mankind: the king of N_2 fixation in the bisophere

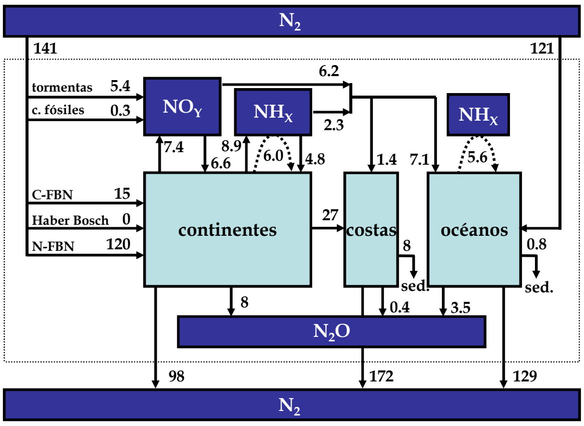

balance global del nitrógeno en 1860 (en Tg N a^{-1})

Galloway et al., Biogeochemistry, 2004

global change and nitrogen in the oceans

mankind: the king of N_2 fixation in the bisophere

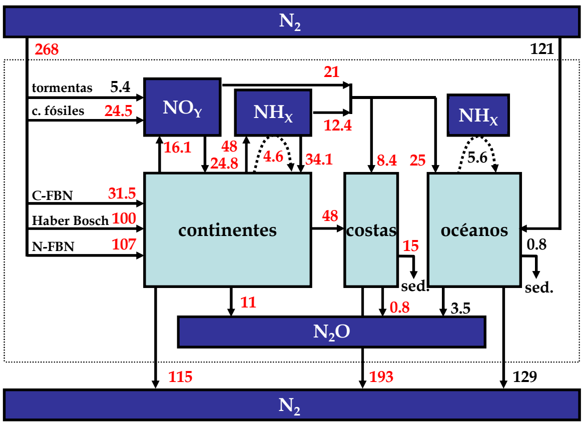

balance global del nitrógeno en 1990 (en Tg N a^{-1})

Galloway et al., Biogeochemistry, 2004

global change and nitrogen in the oceans

mankind: the king of N_2 fixation in the bisophere

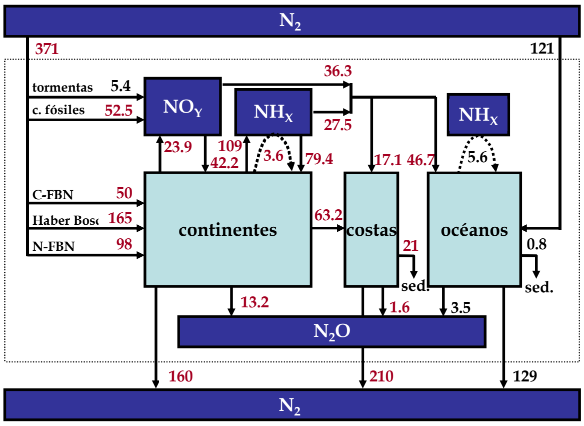

balance global del nitrógeno en 2050 (en Tg N a^{-1})

Galloway et al., Biogeochemistry, 2004

global change and nitrogen in the oceans

deposition of combined nitrogen in the open ocean

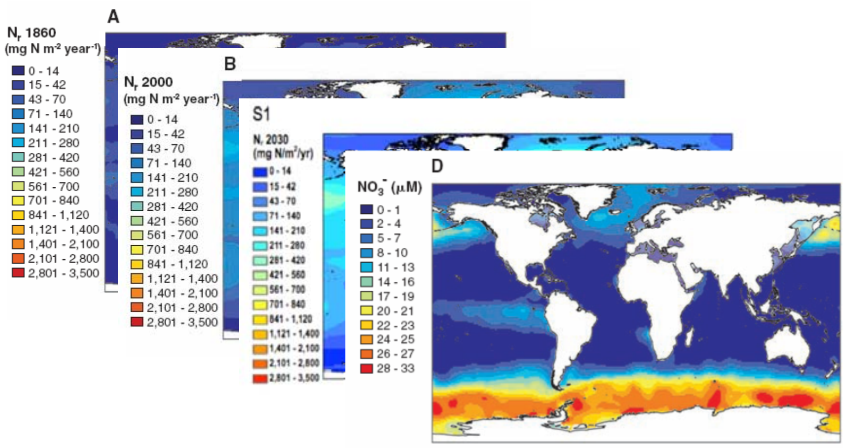

deposition of NHx + NOy + Norg (in Tg N a^{-1})

Duce et al, Science, 2008

global change and nitrogen in the oceans

consequences of the anthropogenic fertilization of the oceans

Table 2. Atmospheric nitrogen deposition to the ocean in 2000 and its impact on productivity. Global-scale estimates of total primary production (*23*); new production (*24–26*); N_2 fixation (*2*, *6–8*). Most letters in italics refer to flux pathways in Fig. 2.

	Global ocean nitrogen (Tg N year^{-1})	Resultant global ocean productivity (Pg C year^{-1})
Total primary production (*a*+*b*+*c*+*d*)	~8800 (7000–10,500)	~50 (40–60)
New production (NP) (*b*)	~1900 (1400–2600)	~11 (8–15)
Marine N_2 fixation (*c*)	~100 (60–200)	~0.57 (0.3–1.1)
Total net N_r deposition (*d*) (NO_y+NH_x+Org. N_r)	~67 (38–96)	~0.38 (0.22–0.55)
Total external nitrogen supply (*c*+*d*)	~167 (98–296)	~0.95 (0.56–1.7)
Anthropogenic N_r deposition (AAN) (*e*)	~54 (31–77)	~0.31 (0.18–0.44)

impact on primary production

Duce et al, Science, 2008

global change and nitrogen in the oceans

consequences of the anthropogenic fertilization of the oceans

Table S1. Estimates of N_2O emission fluxes from oceans in 1860, 2000 and 2030.

	①	②	③	① + ③ = ④	⑤	[②/④] x ⑤ = ⑥	⑥/⑤% = ⑦
Year	N_r (Atmospherically deposited)	N_r (AAN)	N_2 fixation	Total New Fixed N	Total N_2O Emission	Anthro. N_2O Emission	% Anthro. N_2O
1860	20	5.7	100	120	3.6 (2.7-4.5)	0.2 (0.1-0.2)	4.8
2000	67	54	100	167	5.0 (3.8-6.2)	1.6 (1.2-2.0)	32
2030	77	62	100	177	5.3 (4.0-6.6)	1.9 (1.4-2.3)	35

Units are TgNyr^{-1} (except for Column ⑦).

impact on nitrification

Duce et al, Science, 2008

global change and nitrogen in the oceans

consequences of the anthropogenic fertilization of the oceans

Table 1 | Estimates of anthropogenic emissions of nitrous oxide (Tg N_2O-N yr^{-1}).

Source	Mosier *et al.* 1998 (ref. 3)	EPA 2006 (ref. 14)	Crutzen *et al.* 2007 (ref. 7)	This study
Direct emissions from fertilizer on soils	1.5 (0.2-2.7)			
Indirect fertilizer emissions: atmospheric deposition	0.3 (0.06-0.6)	4.4		2.2 (1.5-2.4)
Indirect fertilizer emissions: leaching	1.6 (0.1-7.7)			
Indirect emissions: human sewage	0.2 (0.04-2.6)	0.2	4.3-5.8	Included with fertilizer & manure estimates
Manure: soil applications	0.6 (0.1-1.1)	Included with fertilizer emissions		
Manure: livestock management systems	2.1 (0.6-3.1)	0.4		2.8 (2.2-3.3)
Biomass burning	0.5 (0.2-1.0)	0.6		0.5
Industrial & transport	1.3 (0.7-1.8)	0.8	0.7-1.3	0.8
Total anthropogenic	8.1 (2.1-20.6)	6.3	5.6-6.5	6.3

1 Tg = 10^{12} g. The base year was 1994 for the Mosier *et al.* study and was 2000 for each of the other three studies. The ranges of uncertainty for fertilizer and manure sources in this study (shown in parentheses) are derived from the sensitivity analyses presented in the Supplementary Information.

impact on nitrification

Davidson, Nature Geosciences, 2009

global change and nitrogen in the oceans

consequences of the anthropogenic fertilization of the oceans

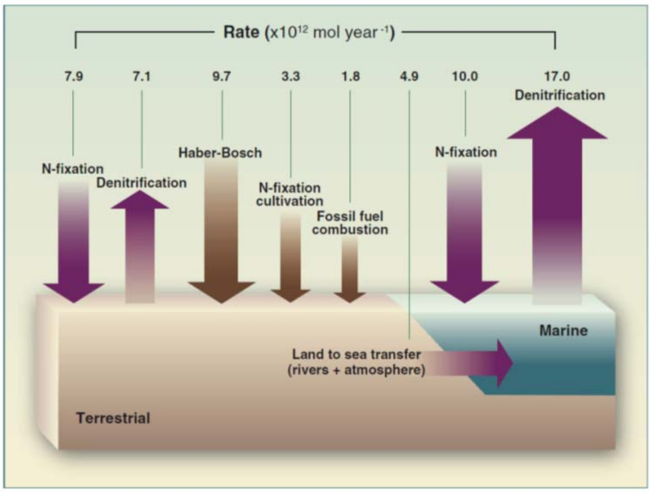

Fig. 4. Rates of nitrogen flux in the modern nitrogen cycle depend on the efficiency of the transformations between reservoirs. Arrow size reflects relative size of the flux. The dark brown arrows represent anthropogenic inputs (*25, 45, 46, 52, 53, 68, 69*).

Canfiled et al, Science, 2010

global change and phosphorus in the oceans

consequences of the anthropogenic fertilization of the oceans

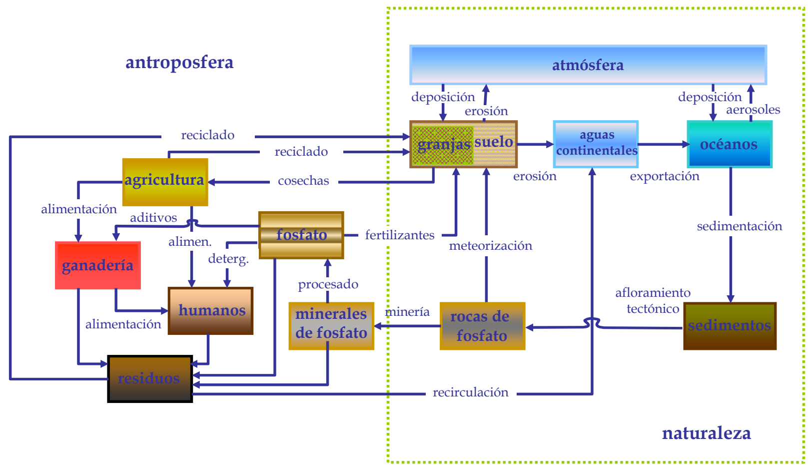

Liu, 2006

global change and phosphorus in the oceans

consequences of the anthropogenic fertilization of the oceans

humankind is …

- ▶ **extracting huge amounts of <u>phosphate</u> from the phosphorite reserves to produce fertilizers**
- ▶ **reducing the <u>phosphate</u> reserves in tropical forests due to deforestation**
- ▶ **adding <u>phosphate</u> to continental and marine aquatic ecosystems**

Liu, 2006

global change and phosphorus in the oceans

consequences of the anthropogenic fertilization of the oceans

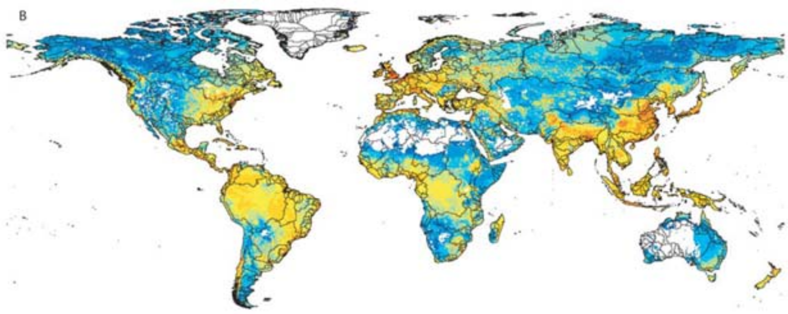

Figure 3. (a) NEWS-DIP-predicted and (b) NEWS-DIP-HD-predicted DIP yield by half-degree grid cell (kg P km^{-2} yr^{-1}). White areas are either endoreic (Figure 3a) or have a predicted DIP loading to surface waters equal to zero (Figure 3b).

Harrison et al, Global Biogeochem Cy, 2010

global change and phosphorus in the oceans

consequences of the anthropogenic fertilization of the oceans

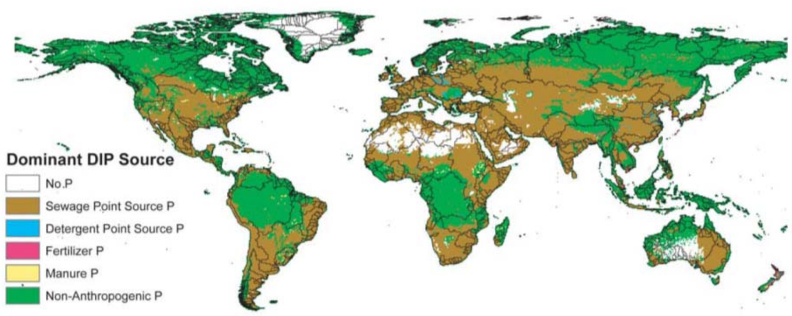

Figure 5. Dominant source of DIP by half-degree grid cell. "Dominant source" is defined as the modeled source that NEWS-DIP-HD predicts contributes the largest single fraction of DIP to the coast.

Harrison et al, Global Biogeochem Cy, 2010

global change and phosphorus in the oceans

consequences of the anthropogenic fertilization of the oceans

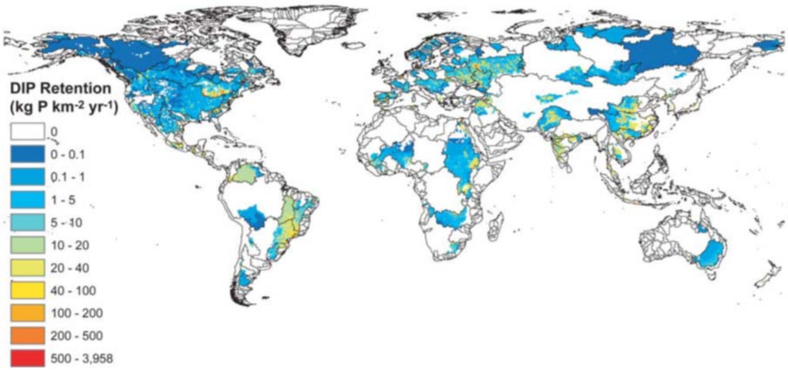

Figure 4. NEWS-DIP-HD-estimated DIP retention (kg P km^{-2} yr^{-1}) globally by half degree. Estimates without information regarding reservoir locations and consumptive water use were assumed to retain no DIP, making this quite a conservative estimate of DIP retention within watersheds globally.

Harrison et al, Global Biogeochem Cy, 2010

global change and phosphorus in the oceans

consequences of the anthropogenic fertilization of the oceans

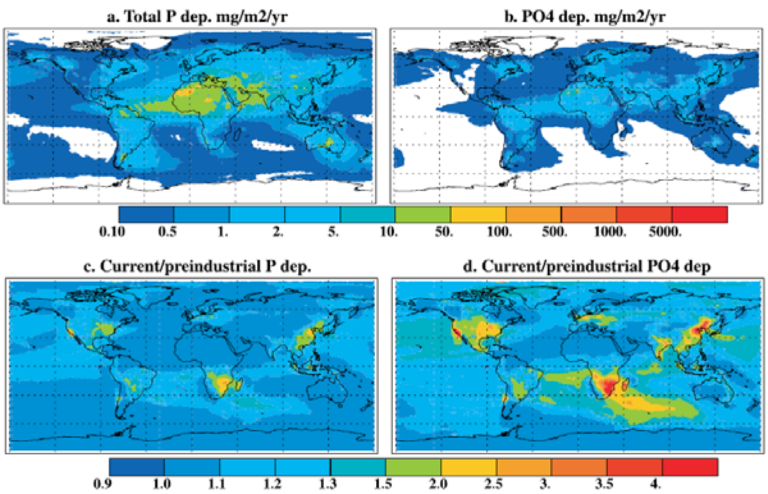

Mahowald et al, Global Biogeochem Cy,2008

global change and phosphorus in the oceans

consequences of the anthropogenic fertilization of the oceans

Table 2 Human intensification of the global phosphorus cycle (all values are in Mt P year^{-1})

Fluxes	Natural	Preindustrial (1800)	Recent (2000)
Natural fluxes intensified by human actions			
Erosion	>10	>15	>30
Wind	<2	<3	>3
Water	>8	>12	>27
River transport	>7	>9	>22
Particulate P	>6	>8	>20
Dissolved P	>1	<2	>2
Biomass combustion	<0.1	<0.2	<0.3
Anthropogenic fluxes			
Crop uptake	–	1	12
Animal wastes	–	>1	>15
Human wastes	–	0.5	3
Organic recycling	–	<0.5	>6
Inorganic Fertilizers	–	–	15

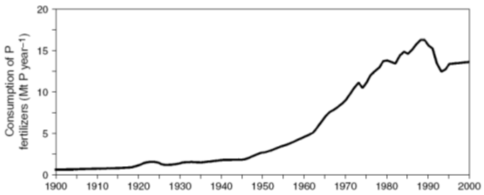

Smil, 2002

global change and phosphorus in the oceans

consequences of the anthropogenic fertilization of the oceans

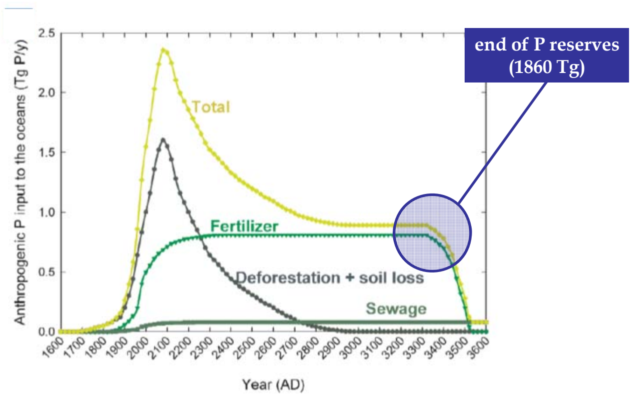

Filippelli, 2008

global change and silicon in the oceans

the decline of diatoms

Humankind is …

- ► **building dams → reduction of silicon discharge**
- ► **transforming virgin into cultured lands → increase of nitrogen discharge**
- ► **warming the Earth → increase of stratification → dinoflagelates dominance**

global change and silicon in the oceans

the decline of diatoms

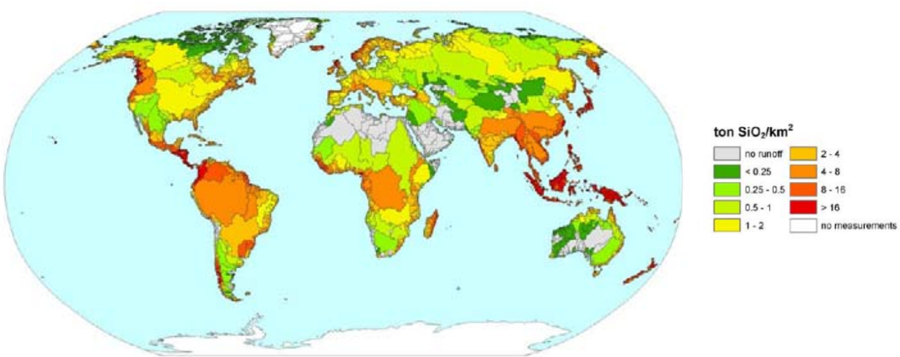

Beunser et al., Global Biogeochemical Cycles, 2009

global change and silicon in the oceans

the decline of diatoms

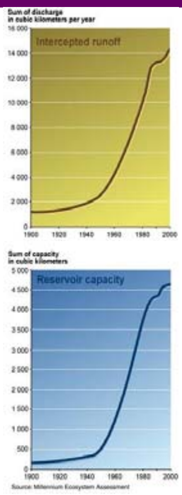

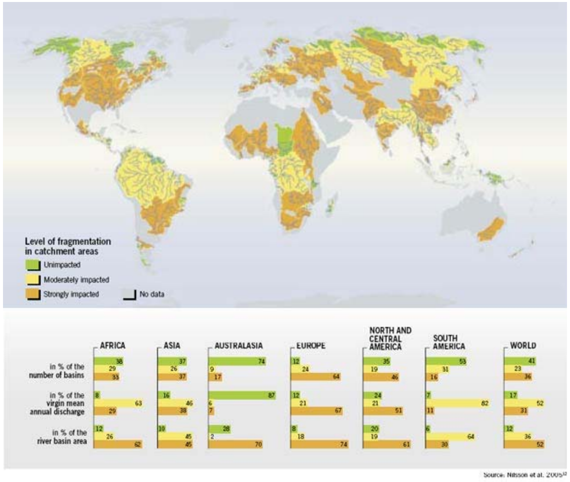

Intercepted runoff is 3 to 6 times natural runoff

http://www.maweb.org.

global change and silicon in the oceans

the decline of diatoms

Table 6. Predicted River Export of DSi to the World's Oceans for the Predam Situation and Retention in Global Reservoirs Based on Two Methods

Ocean	Area (Mkm^2)	Predam DSi River Export ($Tg\ a^{-1}$)	Contribution to Global DSi River Export (%)	DSi Retention With PR[a] (%)	DSi Retention With SR[a] (%)
Arctic Ocean	18	18	5	17	9
Atlantic Ocean	43	155	41	23	25
Indian Ocean	17	51	14	11	11
Land	14	8	2	18	17
Mediterranean + Black Sea	8	11	3	40	46
Pacific Ocean	19	137	36	13	15
World	118	380	100	18	19

[a]PR is the phosphate retention from *Harrison et al.* [2005]; SR is sediment retention from *Vörösmarty et al.* [2003].

River dams retain 20% of the continental dSi that should arrive to the oceans

Beunser et al., Global Biogeochemical Cycles, 2009

global change and silicon in the oceans

the decline of diatoms

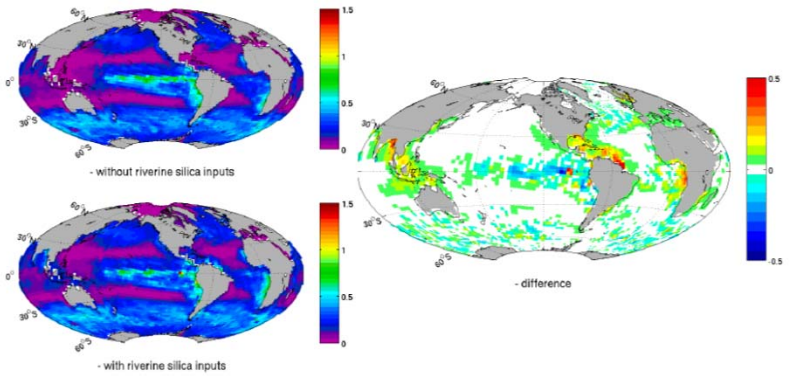

Fig. 5. Rivers contribution to the Opal export production in mol Si m^{-2} $year^{-1}$ – without silica riverine inputs (top-left) – with silica riverine inputs (bottom-left) and the computed difference with/without riverine silica inputs (right).

River dams retain 20% of the continental dSi that should arrive to the oceans

Bernard et al., Biogeosciences, 2010

global change and silicon in the oceans

the decline of diatoms

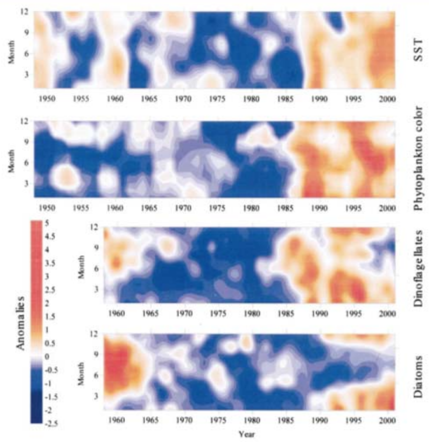

Fig. 1. Monthly standardized anomaly plots for (a) sea surface temperature (1948–2002), (b) phytoplankton color (1948–2002), (c) dinoflagellate cell counts (1958–2002), (d) diatom cell counts (1958–2002). Shades of red signify values above the long-term mean and shades of blue values below the long-term mean. Zero-mean values are in white. Data averaged for the central North Sea.

impact on diatoms biomass in coastal areas

Edwards et al., L&O, 2006

global change and silicon in the oceans

the decline of diatoms

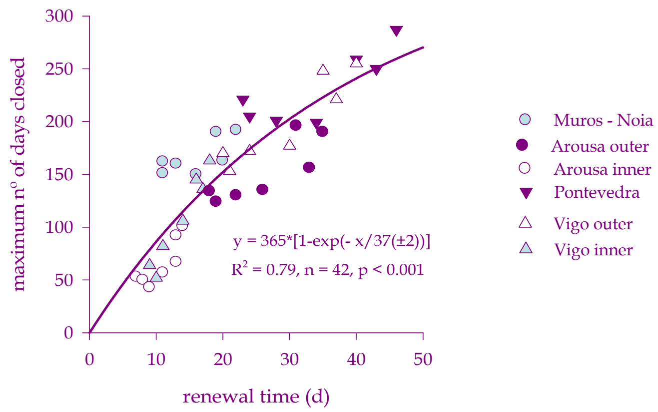

impact on diatoms biomass in coastal areas

Álvarez-Salgado et al., Harmful Algae, 2008

global change and silicon in the oceans

the decline of diatoms

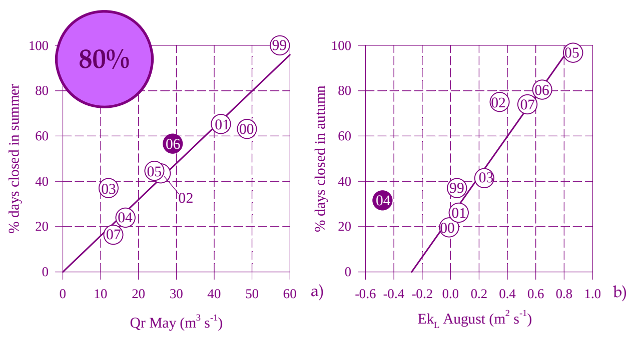

impact on diatoms biomass in coastal areas

Álvarez-Salgado et al., Harmful Algae, 2011